On the range of validity of the fluctuation theorem for stochastic Markovian dynamics

A Rákos[1,2] and R J Harris[3,4]

[1] Department of Physics of Complex Systems, Weizmann Institute of Science, Rehovot 76100, Israel

[2] Research Group for Condensed Matter Physics of the Hungarian Academy of Sciences, Budafoki u. 8, 1111 Budapest, Hungary

[3] Fachrichtung Theoretische Physik, Universität des Saarlandes, 66041 Saarbrücken, Germany

[4] Present Address: School of Mathematical Sciences, Queen Mary, University of London, Mile End Road, London, E1 4NS, United Kingdom

E-mail: rakos@phy.bme.hu, rosemary.harris@qmul.ac.uk

Abstract. We consider the fluctuations of generalized currents in stochastic Markovian dynamics. The large deviations of current fluctuations are shown to obey a Gallavotti-Cohen (GC) type symmetry in systems with a finite state space. However, this symmetry is not guaranteed to hold in systems with an infinite state space. A simple example of such a case is the Zero-Range Process (ZRP). Here we discuss in more detail the already reported [1] breakdown of the GC symmetry in the context of the ZRP with open boundaries and we give a physical interpretation of the phases that appear. Furthermore, the earlier analytical results for the single-site case are extended to cover multiple-site systems. We also use our exact results to test an efficient numerical algorithm of Giardinà, Kurchan and Peliti [2], which was developed to measure the current large deviation function directly. We find that this method breaks down in some phases which we associate with the gapless spectrum of an effective Hamiltonian.

Contents

1. Introduction

An important step in the understanding of non-equilibrium systems has been the development of so-called fluctuation theorems [3, 4] which quantify irreversibility by relating the probability of some "backward" process to that of a corresponding "forward" process. Formally, these fluctuation relationships all derive from a statement about the relative probabilities of a trajectory in phase space and the time-reversed trajectory. The various theorems found in the literature can be divided into two broad classes: transient relations (which are exact for finite times) and steady-state relations (which hold only asymptotically in the long-time limit)—see, e.g., [5, 6] for recent discussion of the various interconnections. In the present paper we will mainly be interested in asymptotic symmetries, specifically whether (or not) a given quantity satisfies a relation of the form

$$\frac{\mathcal{P}(-r,t)}{\mathcal{P}(r,t)} \sim \mathrm{e}^{-rt}. \tag{1}$$

Here $\mathcal{P}(r,t)$ is the probability to observe, over time interval $[0,t]$, a time-averaged value $r \equiv R/t$ of some time-extensive quantity R (e.g., entropy production). The symbol

$\sim$ means logarithmic equality in the limit of large t. In this paper, we refer to the relationship (1) as "the Gallavotti-Cohen fluctuation theorem" or simply "the fluctuation theorem".

Historically, the concept of a fluctuation theorem emerged from computer simulations investigating the entropy production fluctuations in a sheared fluid [7]. A rigorous derivation of the form (1) was then given for the steady state of deterministic systems [8, 9] where the entropy-like functional r can be identified with the rate of phase space contraction. Later proofs addressed stochastic dynamics [10, 11], leading to a general property of the large deviation function sometimes referred to as "Gallavotti-Cohen symmetry" (or GC symmetry for short). Here r is associated with a current of some quantity through the system (e.g., the particle current in a lattice gas) and, for bounded state-space, the relation (1) holds for arbitrary initial condition. Recent work by Kurchan [12] has also explored how to recast the deterministic fluctuation theorem as the vanishing-noise limit of the stochastic one. In parallel to the theoretical development there has been much successful work on experimental verification of fluctuation theorems; for reviews see [4, 13, 14]. In particular, we note that recent experiments using an optical defect in diamond provide a simple realization of a two-state stochastic system [15, 16].

Very recently there has been considerable theoretical, experimental and numerical interest in cases where the symmetry (1) breaks down, see e.g., [17, 18, 19, 20, 1, 21, 22]. It is now understood that this effect can be attributed to certain boundary terms which become relevant in the case of infinite state space; see section 2 below for a detailed exposition in the context of stochastic Markovian dynamics. For deterministic systems, the effect of unbounded potentials was discussed by Bonetto *et al.* [20]. They argued for the restoration of the symmetry by removal of the "unphysical" singular terms. Earlier a similar phenomenon was found for a model of a trapped-Brownian particle treated via a Langevin equation [17, 23]. Within the Langevin framework, discussion of some related subtleties can also be found in [24, 25].

In [1] we provided a general discussion of this breakdown of Gallavotti-Cohen symmetry for *many-particle* stochastic dynamics within the context of a particular model—the zero-range process (ZRP). The ZRP plays a paradigmatic role in non-equilibrium statistical mechanics, hence such work offers a contribution to general understanding as well as providing concrete results for an important model. In the present paper, we give details of the analytical calculations leading to those results and compare them with direct evaluation of the current large deviation function using the recent algorithm of Giardinà, Kurchan and Peliti [2]. We also discuss some generalizations and present new results for the multi-site ZRP.

Interestingly, in the zero-range process, we do not find a constant value for the ratio of probabilities for large forward and backward current fluctuations. This is in stark contrast to analytical arguments [17, 20, 25] and numerical work [21] for other models. We argue below that the failure to observe this form of "extended fluctuation theorem" is due to strong correlations in our model between the boundary terms and the integrated

current. These correlations persist even in the long-time limit; it would be interesting to see if effects of this type can be observed in any experimental situations.

The plan of the rest of the paper is as follows. First, in section 2, we give a general derivation of the Gallavotti-Cohen fluctuation theorem for stochastic systems and indicate also the relation to transient fluctuation theorems. Then, in section 3, we introduce our zero-range model and outline its treatment within this general framework. section 4 is devoted to a detailed calculation of the current large deviation function for the single-site version of this model, giving a concrete example of the breakdown of GC symmetry. In section 5 the analytical approach is complemented by use of the algorithm of [2] to obtain new numerical results for the large deviation function (and general insight into the applicability of the "cloning" method). Significantly, in section 6 we extend our discussion to larger systems, demonstrating how information about the current fluctuations in an L-site ZRP can be obtained by mapping to an effective single-site model. Section 7 contains some conclusions and general perspectives.

2. The fluctuation theorem for Markovian dynamics

2.1. Central argument

Here we present a derivation of the fluctuation theorem for generalized currents of Markov processes defined on a finite configuration space. Our argument is based on that of [11].

Consider a continuous time Markov process which satisfies detailed balance in the stationary state. The system can be described by the transition rates $w^{\rm eq}_{\sigma'\sigma}$ from configuration σ to σ'. In addition, consider a counter J, the value of which increases by the amount $\Theta_{\sigma'\sigma}$ at each transition $\sigma \to \sigma'$. Here the matrix Θ, which is required to be real and antisymmetric, can describe any type of real or abstract current in the system. As an example one can consider the particle current through a given bond: in this case $\Theta_{\sigma'\sigma}$ is the number of particles hopping across the bond at a transition $\sigma \to \sigma'$ (which can be positive or negative depending on the direction of hopping). At $t = 0$ the counter J is set to zero; for any positive time it is a functional acting on the paths (sequences of configurations) from time 0 to time t and can be written as

$$J(t, \{\sigma\}) = \sum_{k=1}^{n-1} \Theta_{\sigma_{k+1}\sigma_k}. \tag{2}$$

Here n is the number of configurations σ_k visited during time t. In the following we refer to J as the "time-integrated current" (or, where no confusion can arise, simply as the "current"). Note that, due to detailed balance, the mean of this current $\langle J(t)\rangle$ is always zero in equilibrium.

We define the driven system by the modified transition rates

$$w_{\sigma'\sigma} = w^{\rm eq}_{\sigma'\sigma} {\rm e}^{\frac{E}{2}\Theta_{\sigma'\sigma}} \tag{3}$$

from configuration σ to σ', where E is a driving field conjugated to the specific current under consideration. In what follows we show that in this driven system the probability distribution function $\mathcal{P}(J,t)$ of the random variable $J(t)$ satisfies the relation

$$\frac{\mathcal{P}(J,t)}{\mathcal{P}(-J,t)} \sim \mathrm{e}^{EJ} \tag{4}$$

asymptotically for large times, provided the state space (i.e., the number of possible configurations) is finite. Here the power EJ can be interpreted as the work done on the system by the external field. This is the statement of the fluctuation theorem.

In cases where the sum $\sum_n \Theta_{\sigma_n,\sigma_{n+1}}$ gives zero for all periodic paths σ_n in the configuration space, J becomes a simple function of the initial and final configuration, i.e., there is no real dependence on the history. In this special case not only the original but also the above-defined "driven" system would satisfy detailed balance in the stationary state. In the following we assume that this is not the case, i.e., there are periodic paths in the configuration space for which the sum $\sum_n \Theta_{\sigma_n,\sigma_{n+1}}$ is non-zero.

For a given *non-equilibrium* model with rates $w_{\sigma'\sigma}$ one can apply a reversed argument. In this case physically one can think of E as a negative driving field, conjugated to the current under consideration, which is needed in order to "restore" detailed balance. If, for a specific value of E, the rates $w^{\mathrm{eq}}_{\sigma'\sigma}$ (defined by (3)) lead to detailed balance then the fluctuation relation (4) holds for this current. This gives some freedom for the quantity J which enters the fluctuation relation. The action functional of [11] (W in that paper) corresponds to the specific choice $\Theta_{\sigma'\sigma} = \ln \frac{w_{\sigma'\sigma}}{w_{\sigma\sigma'}}$ with $E = 1$, which leads to $w^{\mathrm{eq}}_{\sigma'\sigma} = \sqrt{w_{\sigma'\sigma} w_{\sigma\sigma'}}$. These rates indeed lead to detailed balance, since for each pair of configurations the forward and backward transition rates are equal. This also implies that in the corresponding equilibrium distribution every configuration has the same weight.

Let us now define the rate $w(\{\sigma\})$ for a full path as

$$w(\{\sigma\}) = w_{\sigma_1\sigma_0} w_{\sigma_2\sigma_1} \cdots w_{\sigma_n\sigma_{n-1}} \mathrm{e}^{-\frac{t_0}{\tau_0}} \mathrm{e}^{-\frac{t_1-t_0}{\tau_1}} \cdots \mathrm{e}^{-\frac{t-t_{n-1}}{\tau_n}}, \tag{5}$$

where t_k denotes the time when the transition from configuration σ_k to σ_{k+1} happened and $\tau_k = \left(\sum_{\sigma'} w_{\sigma'\sigma_k}\right)^{-1}$ corresponds to the overall exit rate from configuration σ_k. The conditional probability of such a path with transition times between t_k and $t_k + dt$, provided at time 0 the system starts in configuration σ_0 is $w(\{\sigma\})dt^{n-1}$. Using (3) one can readily show that

$$\frac{p^{\mathrm{eq}}_{\sigma_0} w(\{\sigma\})}{p^{\mathrm{eq}}_{\sigma_n} w\left(\{\sigma\}^{\mathrm{rev}}\right)} = \mathrm{e}^{EJ(t,\{\sigma\})}, \tag{6}$$

where $\{\sigma\}^{\mathrm{rev}}$ is the time-reversed path of $\{\sigma\}$ and p^{eq}_σ is the equilibrium probability of configuration σ. In reference [26] the above relation is referred to as the "non-equilibrium detailed balance condition" with EJ being the work done on the system. This also suggests the identification of EJ as the work.

We note that in the case of discrete time dynamics the above scenario is very similar, the only difference is that here the quantities $w_{\sigma'\sigma}$ and $w(\{\sigma\})$ denote transition

probabilities rather than rates and the exponential factors in (5) are replaced by diagonal elements of the transition matrix w.

2.2. Proof of the asymptotic fluctuation theorem for finite systems

In the calculation we use the so-called quantum Hamiltonian formalism where a basis vector is associated with each possible configuration and the state of the system (a probability measure on the configuration space) is denoted by a vector $|P\rangle$ in this space with the normalization $\langle s|P\rangle = 1$. Here $\langle s|$ is a row vector with components $(1, 1, 1, \ldots)$. In this formalism the master equation takes the form

$$\frac{\partial}{\partial t}|P\rangle = -H|P\rangle, \tag{7}$$

which is similar to the Schrödinger equation in imaginary time. The transition rates are in the off-diagonal elements of H and the conservation of probability requires

$$\langle s|H = 0. \tag{8}$$

For more details on this formalism see [27].

As a first step of the proof we introduce the joint probability distribution function $\mathcal{P}_\sigma(J,t)$, which denotes the probability of being in configuration σ and having the value J of the current at time t. In what follows we calculate the generating function $\langle \mathrm{e}^{-\lambda J(t)}\rangle$.

$$\left\langle \mathrm{e}^{-\lambda J(t)} \right\rangle = \langle s|g(t)\rangle\,, \tag{9}$$

where

$$g(t)_\sigma = \sum_J \mathcal{P}_\sigma(J,t)\mathrm{e}^{-\lambda J}. \tag{10}$$

The time derivative of $g(t)$ is

$$\begin{aligned}
\frac{\mathrm{d}}{\mathrm{d}t}g(t)_\sigma &= \sum_J \sum_{\sigma'} \left(\mathcal{P}_{\sigma'}(J-\Theta_{\sigma\sigma'},t)w_{\sigma\sigma'} - \mathcal{P}_\sigma(J,t)w_{\sigma'\sigma}\right)\mathrm{e}^{-\lambda J} \\
&= \sum_{J'} \sum_{\sigma'} \mathcal{P}_{\sigma'}(J',t)w_{\sigma\sigma'}\mathrm{e}^{-\lambda J'}\mathrm{e}^{-\lambda\Theta_{\sigma\sigma'}} - g(t)_\sigma \sum_{\sigma'} w_{\sigma'\sigma} \\
&= \sum_{\sigma'} g(t)_{\sigma'} w_{\sigma\sigma'}\mathrm{e}^{-\lambda\Theta_{\sigma\sigma'}} - g(t)_\sigma \sum_{\sigma'} w_{\sigma'\sigma} \\
&= -\tilde{H}(\lambda)_{\sigma\sigma'} g(t)_{\sigma'},
\end{aligned} \tag{11}$$

where $\tilde{H}(\lambda)$ is a modified Hamiltonian in which the transition rates corresponding to $\sigma' \to \sigma$ are multiplied by the factor $\mathrm{e}^{-\lambda\Theta_{\sigma\sigma'}}$. Note that $\tilde{H}(\lambda)$ is a non-stochastic matrix with $\langle s|\tilde{H}(\lambda) \neq \langle s|$ for $\lambda \neq 0$. Since $|g(0)\rangle$ is identical to the initial measure $|P_0\rangle$ the generating function takes the form

$$\left\langle \mathrm{e}^{-\lambda J(t)} \right\rangle = \left\langle s \left| \mathrm{e}^{-\tilde{H}(\lambda)t} \right| P_0 \right\rangle. \tag{12}$$

The long-time behaviour of this quantity is characterized by the function

$$e(\lambda) = -\lim_{t\to\infty} \frac{1}{t} \ln \left\langle \mathrm{e}^{-\lambda J(t)} \right\rangle. \tag{13}$$

One finds from (12) that as long as the configuration space is finite, $e(\lambda)$ is given by the lowest eigenvalue $\epsilon_0(\lambda)$ of $\tilde{H}(\lambda)$, since

$$\left\langle \mathrm{e}^{-\lambda J(t)} \right\rangle = \sum_i \langle s|\psi_i\rangle \langle \psi_i|P_0\rangle \, \mathrm{e}^{-\epsilon_i(\lambda)t} \simeq \langle s|\psi_0\rangle \langle \psi_0|P_0\rangle \, \mathrm{e}^{-\epsilon_0(\lambda)t}, \tag{14}$$

Where $\epsilon_i(\lambda)$ are the eigenvalues and ψ_i are the eigenvectors of $\tilde{H}(\lambda)$. It is easy to show that $e(\lambda)$ is related to the large deviation function

$$\hat{e}(j) = -\lim_{t\to\infty} \frac{1}{t} \ln \mathcal{P}(tj,t) \tag{15}$$

of the time-averaged current $j = J/t$ through a Legendre transformation:

$$\hat{e}(j) = \max_\lambda \{e(\lambda) - \lambda j\}, \qquad e(\lambda) = \min_j \{\hat{e}(j) + \lambda j\}. \tag{16}$$

As a second step in the proof we show that $\tilde{H}$ has the symmetry property

$$\tilde{H}(\lambda)^T = P_{\mathrm{eq}}^{-1} \tilde{H}(E-\lambda) P_{\mathrm{eq}}, \tag{17}$$

where P_{eq} is a matrix with the equilibrium probabilities p_σ^{eq} on the diagonal and zero elsewhere. For the rhs of (17) one finds

$$\left[P_{\mathrm{eq}}^{-1} \tilde{H}(E-\lambda) P_{\mathrm{eq}}\right]_{\sigma'\sigma} = -w_{\sigma'\sigma} \mathrm{e}^{-(E-\lambda)\Theta_{\sigma'\sigma}} \frac{p_\sigma^{\mathrm{eq}}}{p_{\sigma'}^{\mathrm{eq}}} (1-\delta_{\sigma'\sigma}) + \sum_\rho w_{\rho\sigma}\delta_{\sigma'\sigma}, \tag{18}$$

which leads to

$$w_{\sigma\sigma'} \mathrm{e}^{-\lambda\Theta_{\sigma\sigma'}} = w_{\sigma'\sigma} \mathrm{e}^{-(E-\lambda)\Theta_{\sigma'\sigma}} \frac{p_\sigma^{\mathrm{eq}}}{p_{\sigma'}^{\mathrm{eq}}} \tag{19}$$

for the non-diagonal elements of equality (17). Using (3) and the fact that the matrix Θ is antisymmetric, the above condition takes the form

$$w_{\sigma\sigma'}^{\mathrm{eq}} p_{\sigma'}^{\mathrm{eq}} = w_{\sigma'\sigma}^{\mathrm{eq}} p_\sigma^{\mathrm{eq}}, \tag{20}$$

which is just the detailed balance condition for the equilibrium system and is trivially satisfied. This proves the relation (17) (The diagonal part of both the lhs and rhs is just the diagonal part of the original non-equilibrium Hamiltonian.)

As a corollary of the symmetry property (17) one finds the important relation

$$e(\lambda) = e(E-\lambda). \tag{21}$$

For the large deviation function $\hat{e}(j)$, using the Legendre transformation (16) this implies

$$\hat{e}(-j) = Ej + \hat{e}(j), \tag{22}$$

which is equivalent to (4).

2.3. Transient fluctuation theorem

The relation (4) is true only asymptotically, for large times. However, due to the symmetry (17), one can show that for specific initial conditions it can be made exact for any finite time. Namely, taking the equilibrium distribution $|p^{\rm eq}\rangle$ as the initial condition then for the generating function one finds

$$\begin{aligned}\langle {\rm e}^{-\lambda J(t)}\rangle &= \langle s|{\rm e}^{-\tilde{H}(\lambda)t}|p^{\rm eq}\rangle = \langle p^{\rm eq}|{\rm e}^{-\tilde{H}(\lambda)^T}|s\rangle = \langle p^{\rm eq}|P_{\rm eq}^{-1}{\rm e}^{-\tilde{H}(E-\lambda)t}P_{\rm eq}|s\rangle \\ &= \langle s|{\rm e}^{-\tilde{H}(E-\lambda)t}|p^{\rm eq}\rangle = \langle {\rm e}^{-(E-\lambda)J(t)}\rangle. \end{aligned} \tag{23}$$

This implies that the relation (4) holds exactly for any finite time (but only for this specific initial condition). This is the statement of the transient fluctuation theorem of Evans and Searles [28, 29, 3].

2.4. Boundary terms

As mentioned above, in a non-equilibrium system one has some freedom to choose the current to be considered. Here we investigate whether two different choices really give two independent relations for the fluctuations of the non-equilibrium system. In order to satisfy the conditions of the theorem, by applying $-E$ field in the non-equilibrium model one should get back to detailed balance, which can be formulated as

$$\frac{w_{\sigma\sigma'}{\rm e}^{-\frac{E}{2}\Theta_{\sigma\sigma'}}}{w_{\sigma'\sigma}{\rm e}^{-\frac{E}{2}\Theta_{\sigma'\sigma}}} = \frac{{\rm e}^{-V_\sigma}}{{\rm e}^{-V_{\sigma'}}}. \tag{24}$$

Here V_σ is the energy of configuration σ in the equilibrium system. Taking the logarithm of (24) and summing up for a path results in

$$J^*(t) - EJ(t) = V_{\sigma_{\rm ini}} - V_{\sigma_{\rm fin}}, \tag{25}$$

where J^* is the action functional of [11] and $V_{\sigma_{\rm ini(fin)}}$ is the potential in the initial (final) state. This shows that any two currents (that satisfy the conditions of the fluctuation theorem) differ only in boundary terms. In finite systems these terms are bounded, consequently their contribution to the net current is negligible in the limit, where $t \to \infty$. In these systems the fluctuation theorems for different currents give essentially the same information.

In order to demonstrate this, consider a driven exclusion process on a finite lattice. Here the number of possible configurations is clearly finite. There are many ways of defining the integrated particle current in the system: one can consider the current through a given bond, take a space-averaged current or measure the distance travelled by a tagged particle (in periodic systems). All these definitions give a different current for finite times but in the $t \to \infty$ limit they are essentially the same, since the difference between them is bounded while they are proportional to t.

However, for systems with infinite configuration space this argument does not hold and the boundary terms can be relevant even for large times, leading to several independent relations for the fluctuations.

The fact that the difference between two currents can be written as a boundary term suggests that the same holds for the difference between two initial states. Suppose that the transient fluctuation theorem holds for $J^{(1)}, E^{(1)}$ with the initial measure $p_\sigma^{\mathrm{eq}(1)} = \mathrm{e}^{-V_\sigma^{(1)}}$. Since for any two currents $E^{(1)}J^{(1)} = E^{(2)}J^{(2)} + V^{(2)}_{\sigma_{\mathrm{ini}}} - V^{(2)}_{\sigma_{\mathrm{fin}}} - V^{(1)}_{\sigma_{\mathrm{ini}}} + V^{(1)}_{\sigma_{\mathrm{fin}}}$, the transient fluctuation theorem holds for any current J with a boundary term as

$$J_{\mathrm{corr}} = EJ + V_{\sigma_{\mathrm{ini}}} - V_{\sigma_{\mathrm{fin}}} - V^{\mathrm{ini}}_{\sigma_{\mathrm{ini}}} + V^{\mathrm{ini}}_{\sigma_{\mathrm{fin}}}, \tag{26}$$

where V is the equilibrium potential corresponding to the current J and $V^{\mathrm{ini}}_\sigma = \ln p^{\mathrm{ini}}_\sigma$ with p^{ini}_σ being the initial measure (J_{corr} satisfies the theorem with $E = 1$).

2.5. Breakdown of the fluctuation theorem in infinite systems

For infinite systems the above argument breaks down at (14), where one identifies $e(\lambda)$ defined in (13) with the lowest eigenvalue of $\tilde{H}(\lambda)$. In cases where $\tilde{H}$ is infinite-dimensional, there is no guarantee that the scalar products appearing in (14) are finite. An explicit example of this breakdown is given in [1] and will be discussed in detail below. Note however, that the derivation of the transient fluctuation theorem still holds even for infinite systems. Consequently, a violation of the asymptotic fluctuation theorem requires the unbounded growth of the boundary term in (26).

To avoid possible confusion, we remark here that in the original dynamical systems formulation [8, 9] of the GC symmetry, a critical value r^* already appears above which the relation (1) does not hold. This is a direct consequence of the fact that the large deviation function (equivalent to $\hat{e}$ in our notation) diverges outside a finite interval. In contrast, in the stochastic framework of this paper, we consider situations where the large deviation function is always finite (i.e., formally $r^* = \infty$) but the symmetry may still have a restricted range of validity due to the relevance of boundary terms. Indeed, it has also recently been understood in the dynamical systems context, that adding singular boundary terms to a system with finite r^* leads to a further reduction in the symmetry regime, see [20].

2.6. Extended fluctuation theorem

The argument we present in this section is largely based on that of van Zon and Cohen [17, 23], where they describe a generic scenario for the breakdown of the fluctuation theorem in the context of Langevin dynamics. This leads to an "extended fluctuation theorem", where the quantity $\hat{e}(j) - \hat{e}(-j)$ is linear for small j (as suggested by the fluctuation theorem) but, after an intermediate crossover regime, saturates to a constant value for large j. Similar arguments are also given in [25].

Our starting point is equation (26) which we now write for the time-intensive quantities:

$$j_{\mathrm{corr}} = j + t^{-1}(B_{\mathrm{ini}} - B_{\mathrm{fin}}). \tag{27}$$

Here j_{corr} is the corrected current for which the fluctuation theorem holds, and B is a boundary term, which depends only on the initial/final configuration of the history.

First we assume that the probability distribution $\mathcal{P}_{(B)}$ of B has an exponential tail for very large/small values of B:

$$\mathcal{P}_{(B)}(B,t) \sim \begin{cases} \mathrm{e}^{-A^+B} & B \to \infty \\ \mathrm{e}^{A^-B} & B \to -\infty \end{cases} . \tag{28}$$

Here we set $A^{+/-}$ to infinity if B is bounded from above/below. Focusing on the case where the initial state is the steady state, one can assume that the probability distribution of B is identical for the initial and final state, moreover, for large measurement times they become independent. This implies that the probability distribution of

$$b = t^{-1}(B_{\mathrm{ini}} - B_{\mathrm{fin}}) \tag{29}$$

is of the form

$$\mathcal{P}_{(b)}(b,t) \sim \mathrm{e}^{-tA|b|}, \tag{30}$$

where $A = \min(A^+, A^-)$.

As a next step we assume that b and j_{corr} as random variables are independent. In this case the large deviation function of the fluctuations of $j = j_{\mathrm{corr}} + b$ are determined by

$$\hat{e}(j) = \min_{j_{\mathrm{corr}}}(\hat{e}_{\mathrm{c}}(j_{\mathrm{corr}}) + A|j_{\mathrm{corr}} - j|). \tag{31}$$

Here $\hat{e}_{\mathrm{c}}$, which describes the large deviations of j_{corr}, satisfies the fluctuation theorem, i.e., $\hat{e}_{\mathrm{c}}(-j) - \hat{e}_{\mathrm{c}}(j) = j$. In figure 1, one can see how $\hat{e}(j)$ can be obtained from $\hat{e}_{\mathrm{c}}(j)$ graphically by using (31). The points $-j_1$ and j_2 are defined as those values of j where the derivative of the convex function $\hat{e}_{\mathrm{c}}(j)$ becomes $-A$ and A respectively. Outside the interval $(-j_1, j_2)$ the function $\hat{e}(j)$ is linear with slope $\pm A$. Consequently, the quantity $\hat{e}(-j) - \hat{e}(j)$ is linear from zero to $j = \min(j_1, j_2)$, and after a crossover regime it saturates at $j = \max(j_1, j_2)$ to a constant value C. We remark that in the case where $e_{\mathrm{c}}(j)$ is symmetric with respect to $\langle j \rangle$ (e.g. in the case of Gaussian fluctuations) $C = 2A\langle j \rangle$.

In a more general situation, where the initial state is not stationary, the fluctuations of B are different in the initial and final state (we still require that the tails are exponential).

$$\mathcal{P}_{(B_{\mathrm{ini}})}(B,t) \sim \begin{cases} \mathrm{e}^{-A^+_{\mathrm{ini}}B} & B \to \infty \\ \mathrm{e}^{A^-_{\mathrm{ini}}B} & B \to -\infty \end{cases} . \tag{32}$$

In this case the large deviations of b take the following form:

$$\mathcal{P}_{(b)}(b,t) \sim \begin{cases} \mathrm{e}^{-tA_1 b} & b > 0 \\ \mathrm{e}^{tA_2 b} & b < 0 \end{cases} , \tag{33}$$

where $A_1 = \min(A^+_{\mathrm{ini}}, A^-)$ and $A_2 = \min(A^-_{\mathrm{ini}}, A^+)$. This leads to a variant of the extended fluctuation theorem, where the the quantity $\hat{e}(-j) - \hat{e}(j)$ does not saturate but becomes linear with a non-zero slope for large j.

We stress that the above argument relies strongly on the assumption that the boundary terms are independent of the bulk contribution. There are various examples in

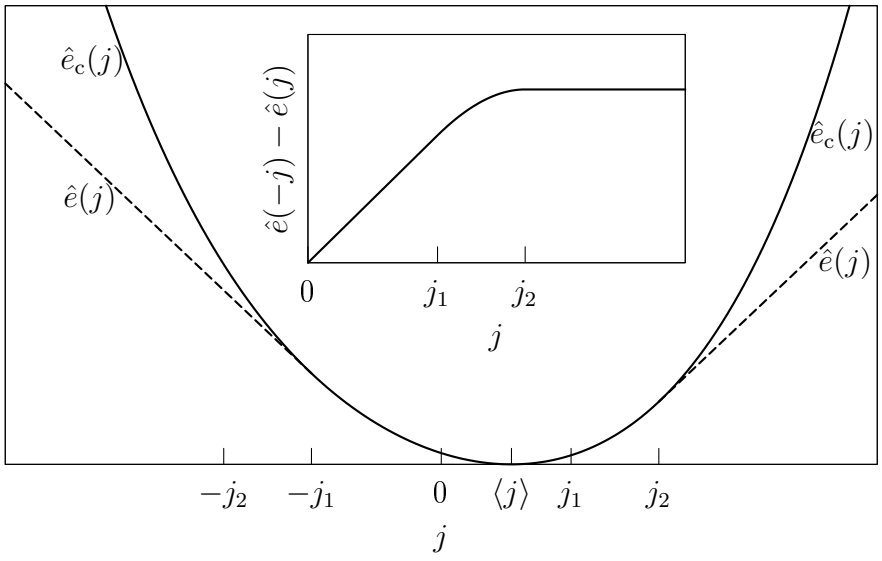

Figure 1. A schematic plot showing the large deviation functions $e(j)$ and $\hat{e}_{\rm c}(j)$. While the fluctuation theorem holds for $e_{\rm c}(j)$, a modified form is found for $\hat{e}(j)$, as plotted in the inset

the literature where this holds, and the above extended form of the fluctuation theorem was found, e.g., [23, 17, 21]. In contrast, in the remainder of this paper, we discuss a simple stochastic Markovian system where there is a strong correlation between the boundary and bulk terms and hence this extended fluctuation theorem is not expected to hold.

3. Zero-range process

Here we demonstrate how the general formalism of the preceding section is applied to a specific model—the zero-range process (ZRP). First introduced by Spitzer in 1970 [30], the ZRP now plays a paradigmatic role in non-equilibrium statistical mechanics, see [31] for a recent review. In particular, for certain choices of parameters the model exhibits a condensation transition [32, 33] in which a macroscopic proportion of particles pile up on a single site. Condensation phenomena are well-known in colloidal and granular systems [34] and also occur in a variety of other physical and non-physical contexts [31].

3.1. Model

We study the one-dimensional partially asymmetric zero-range process with open boundaries [35]—see figure 2. Each lattice site can be occupied by any integer number of particles, the uppermost of which hops randomly to a nearest neighbour site after an exponentially distributed waiting time. In the bulk particles move to the right (left)

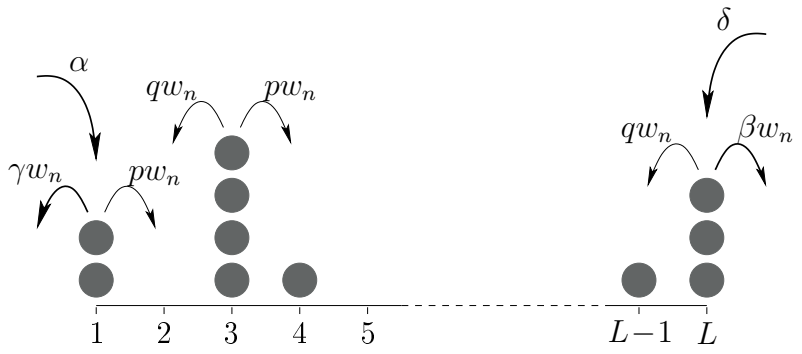

Figure 2. Schematic representation of the ZRP on an open L-site lattice

with rate pw_n (qw_n) where w_n is a function of the number of particles n on the departure site ($w_0 = 0$ by definition). Note that $w_n = n$ would correspond to free particles whereas all other forms represent an attractive or repulsive inter-particle interaction. The top particle on the leftmost lattice site (site 1) leaves the system with rate γw_n whereas new particles are injected with rate α. Correspondingly, on the rightmost site (site L) particles are removed (injected) with rates βw_n (δ). For later convenience we label each bond by the site at its left-hand end, i.e., the lth bond is between sites l and $l+1$.

In the quantum Hamiltonian formalism this dynamics is encoded in the Hamiltonian

$$H = -\Big\{\sum_{l=1}^{L-1}\Big[p(a_l^- a_{l+1}^+ - d_l) + q(a_l^+ a_{l+1}^- - d_{l+1})\Big] + \alpha(a_1^+ - 1) + \gamma(a_1^- - d_1) + \delta(a_L^+ - 1) + \beta(a_L^- - d_L)\Big\} \tag{34}$$

where a^+ and a^- are infinite-dimensional particle creation and annihilation matrices

$$a^+ = \begin{pmatrix} 0 & 0 & 0 & 0 & \cdots \\ 1 & 0 & 0 & 0 & \cdots \\ 0 & 1 & 0 & 0 & \cdots \\ 0 & 0 & 1 & 0 & \cdots \\ \vdots & \vdots & \vdots & \vdots & \ddots \end{pmatrix}, \qquad a^- = \begin{pmatrix} 0 & w_1 & 0 & 0 & \cdots \\ 0 & 0 & w_2 & 0 & \cdots \\ 0 & 0 & 0 & w_3 & \cdots \\ 0 & 0 & 0 & 0 & \cdots \\ \vdots & \vdots & \vdots & \vdots & \ddots \end{pmatrix} \tag{35}$$

and d is a diagonal matrix with the (i,j)th element given by $w_i\delta_{i,j}$.

3.2. Stationary state, current fluctuations

The steady state of the ZRP is given by a product measure (in other words, the stationary distributions for each site are uncorrelated):

$$|P^*\rangle = |P_1^*) \otimes |P_2^*) \otimes \ldots \otimes |P_L^*) \tag{36}$$

where $|P_l^*)$ is the probability vector with components

$$P^*(n_l = n) = \frac{z_l^n}{Z_l}\prod_{i=1}^{n} w_i^{-1}. \tag{37}$$

Here the empty product $n = 0$ is defined equal to 1 and Z_l is the local analogue of the grand-canonical partition function

$$Z_l \equiv Z(z_l) = \sum_{n=0}^{\infty} z_l^n \prod_{i=1}^{n} w_i^{-1}. \tag{38}$$

The fugacities z_l are uniquely determined by the hopping rates α, β, γ, δ, p and q. However, for w_n bounded (i.e., $\lim_{n\to\infty} w_n = a$ with $a < \infty$), Z_l has a finite radius of convergence. For parameters leading to fugacities outside this radius of convergence, a growing boundary condensate occurs [35].

We are interested in the application of the fluctuation theorem to this model, for the case where the boundary parameters are chosen to give a well-defined steady state, i.e., without boundary condensation. As discussed in the preceding section, one can consider a variety of different "currents" through the system. However, since the state space is unbounded (each lattice site can contain an arbitrarily large number of particles) we anticipate the possibility of relevant boundary terms and different fluctuation relationships.

A natural choice is to look at the physical current of particles across a particular bond. For example, suppose we choose to focus on the particle current into the system (i.e., across the 0th bond), then the modified Hamiltonian is given by

$$\begin{aligned}\tilde{H}(\lambda) = -\Big\{ &\sum_{l=1}^{L-1} \left[p(a_l^- a_{l+1}^+ - d_l) + q(a_l^+ a_{l+1}^- - d_{l+1}) \right] \\ &+ \alpha(a_1^+ \mathrm{e}^{-\lambda} - 1) + \gamma(a_1^- \mathrm{e}^{\lambda} - d_1) + \delta(a_L^+ - 1) + \beta(a_L^- - d_L) \Big\}. \end{aligned} \tag{39}$$

In the next section we will examine closely the spectrum of this Hamiltonian for the $L = 1$ single site case. Here we recap some known results for the general L-site case as obtained in [36].

If w_n is unbounded, (i.e., $\lim_{n\to\infty} w_n = \infty$) then $\tilde{H}(\lambda)$ has a gapped spectrum for all λ with lowest eigenvalue given by‡

$$\epsilon_0(\lambda) = \frac{(p-q)(\mathrm{e}^{\lambda}-1)\left[\alpha\beta\left(\frac{p}{q}\right)^{L-1}\mathrm{e}^{-\lambda} - \gamma\delta\right]}{\gamma(p-q-\beta) + \beta(p-q+\gamma)\left(\frac{p}{q}\right)^{L-1}}. \tag{40}$$

The right eigenvector $|\psi_0\rangle$ corresponding to (40) has the same form as the stationary product measure (36) with fugacities

$$z_l = \frac{[(\alpha\mathrm{e}^{-\lambda}+\delta)(p-q) - \alpha\beta\mathrm{e}^{-\lambda} + \gamma\delta]\left(\frac{p}{q}\right)^{l-1} - \gamma\delta + \alpha\beta\mathrm{e}^{-\lambda}\left(\frac{p}{q}\right)^{L-1}}{\gamma(p-q-\beta) + \beta(p-q+\gamma)\left(\frac{p}{q}\right)^{L-1}}. \tag{41}$$

and the left-hand eigenvector is also a product state with one-site marginal "fugacities"

$$\tilde{z}_l = \frac{\beta\gamma(\mathrm{e}^{\lambda}-1)\left(\frac{p}{q}\right)^{L-l} + \gamma\mathrm{e}^{\lambda}(p-q-\beta) + \beta(p-q+\gamma)\left(\frac{p}{q}\right)^{L-1}}{\gamma(p-q-\beta) + \beta(p-q+\gamma)\left(\frac{p}{q}\right)^{L-1}}. \tag{42}$$

‡ The leading order term in an $L \to \infty$ expansion for the bulk-symmetric case, corresponding to the limit $p = q = 1$ in (40), has also been obtained by an additivity principle [37] and by field-theoretic methods [38].

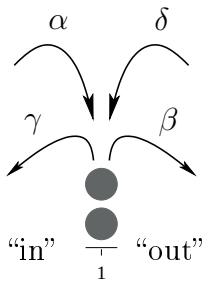

Figure 3. Schematic representation of the single-site ZRP with $w_n = 1$.

Note that this result is independent of the details of w_n and one can also show that it is the same for currents across all bonds meaning that the current fluctuations are spatially homogeneous in the long-time limit. Furthermore the scalar products appearing in equation (14) are finite and the standard Gallavotti-Cohen fluctuation theorem is recovered. Physically, unbounded w_n means that there is no chance for the temporary accumulation of a large numbers of particles on any site.

However, *if w_n is bounded*, then there is a crossover to a gapless spectrum at some value of λ and also the scalar products in equation (14) can be infinite. In fact, $\langle\psi_0|P_0\rangle$ and $\langle s|\psi_0\rangle$ are related to the distribution of initial and final boundary terms and the condition for $\langle\psi_0|P_0\rangle$ to diverge obviously depends on the initial state. Thus, although the symmetry of the eigenvalues remains, we expect the breakdown of the usual Gallavotti-Cohen fluctuation theorem in a spatially homogeneous and initial-condition-dependent way. To explore this issue in more detail we present, in the next section, explicit calculations for the single-site case.

4. Analytical results for single-site model

As a simple example of the ZRP with bounded w_n, we now focus on the single-site model with $w_n = 1$—see figure 3. Even this apparently simple model exhibits a rich phase behaviour, as shown in [1]. One must now distinguish between the particle currents across only two bonds viz. the 0th ("input") and 1st ("output"). Since fluctuations across the two bonds are simply related by left-right reflection, we will consider only the former except where explicitly stated otherwise. Note that the occupation number n of the site performs a random walk on a semi-infinite lattice but with two independent processes for movement in each direction. For a well-defined steady state this random walk should be biased towards the reflecting boundary at $n = 0$, i.e., we require $\alpha + \delta < \beta + \gamma$. If this condition is not met then there is a growing condensate on the site.

Let us first consider an initial Boltzmann distribution given by

$$|P_0\rangle = (1 - x) \sum_{n=0}^{\infty} x^n |n\rangle \tag{43}$$

where $|n\rangle$ denotes the configuration with site occupied by n particles (i.e., a column vector with a '1' in the nth position and '0's elsewhere) and the "fugacity" x is less than

Values of λ	Corresponding values of j
$e^{\lambda_1} \equiv \frac{\alpha}{\beta+\gamma-\delta}$	$j_a \equiv \frac{(\beta+\gamma-\delta)^2-\alpha\gamma}{\beta+\gamma-\delta}$, $j_b \equiv \frac{\beta(\beta+\gamma-\delta)^2-\alpha\gamma\delta}{(\beta+\gamma)(\beta+\gamma-\delta)}$
$e^{\lambda_2} \equiv \frac{(\beta+\gamma)^2-\alpha\gamma-\beta\delta+\eta}{2\gamma\delta}$	$j_c \equiv -\frac{\eta}{\beta+\gamma}$
$e^{\lambda_3} \equiv \frac{\delta-\beta x^2+\sqrt{(\delta-\beta x^2)^2+4\alpha\gamma x^2}}{2\gamma x^2}$	$j_d \equiv \frac{-(\delta-\beta x^2)}{x}$
$e^{\lambda_4} \equiv \frac{\beta(1-x)+\gamma}{\gamma x}$	$j_e \equiv \frac{\alpha\beta\gamma x^2-\delta[\beta(1-x)+\gamma]^2}{x(\beta+\gamma)[\beta(1-x)+\gamma]}$, $j_f \equiv \frac{\alpha\gamma-[\beta(1-x)+\gamma]^2}{\beta(1-x)+\gamma}$

Table 1. Transition values for input current fluctuations in single-site ZRP.

1 for normalization. For example, the choice $x = (\alpha + \delta)/(\beta + \gamma)$ is the steady-state initial condition. Note also that the limit $x \to 0$ corresponds to the empty-site case and that by ergodicity this gives the same result as any fixed particle configuration.

To obtain the large deviations of input current, we need to calculate the matrix element $\langle s|e^{-\tilde{H}t}|P_0\rangle$ where the modified Hamiltonian $\tilde{H}(\lambda)$ is given by

$$\begin{pmatrix} \alpha+\delta & -\gamma e^{\lambda}-\beta & 0 & 0 & \dots \\ -\alpha e^{-\lambda}-\delta & \alpha+\beta+\gamma+\delta & -\gamma e^{\lambda}-\beta & 0 & \dots \\ 0 & -\alpha e^{-\lambda}-\delta & \alpha+\beta+\gamma+\delta & -\gamma e^{\lambda}-\beta & \dots \\ 0 & 0 & -\alpha e^{-\lambda}-\delta & \alpha+\beta+\gamma+\delta & \dots \\ \vdots & \vdots & \vdots & \vdots & \ddots \end{pmatrix} \tag{44}$$

In appendix A.1, we first present an explicit calculation of the spectrum of $\tilde{H}(\lambda)$ and thereby illustrate the crossover to a gapless regime. Then, in appendix A.2, we show how to obtain an integral representation of the matrix element $\langle s|e^{\tilde{H}(\lambda)}|P_0\rangle$ and thus extract the large deviation behaviour. This enables us to construct and explain the "phase diagram" for current fluctuations as shown in section 4.1. Finally, in 4.3 we discuss some straightforward generalizations of these results.

4.1. Phase diagrams

In order to extract the large-time behaviour from the integral representation (A.13) we can use the method of steepest descents with saddle-point at $z = 1$. However, care must be taken due to the poles in the integrands (at $z = \phi^{-1}$, $(\phi x)^{-1}$,ϕ and y). If the saddle-point contour has to be deformed through one of these poles then we must take into account the contribution of the residue at that pole. For a given λ, $e(\lambda)$ is then determined by the term which decays most slowly with t. This yields changes in behaviour at the values of λ given in table 1, where we have defined for convenience the parameter combination

$$\eta = \sqrt{[(\beta+\gamma)^2 - \beta\delta - \alpha\gamma]^2 - 4\alpha\beta\gamma\delta}. \tag{45}$$

Phase A: $\lambda < \lambda_1$ (see figure 4). Here $e(\lambda)$ takes the form

$$e(\lambda) = \alpha\left(1 - e^{-\lambda}\right) + \gamma\left(1 - e^{\lambda}\right), \tag{46}$$

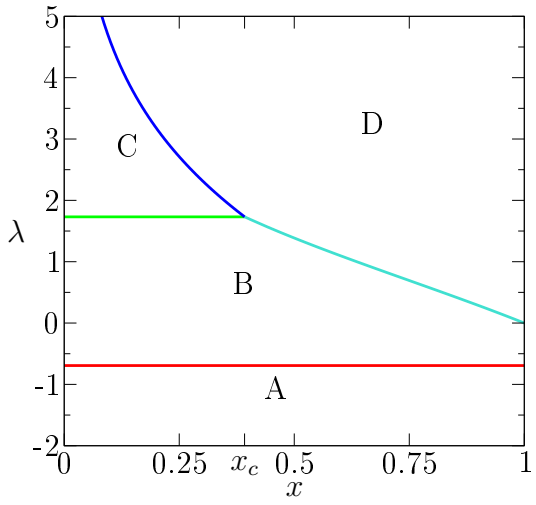

Figure 4. The x–λ phase diagram for $\alpha = \gamma = \delta = 0.1$, $\beta = 0.2$. Red line: $\lambda = \lambda_1$, green line: $\lambda = \lambda_2$, blue line: $\lambda = \lambda_3(x)$, cyan line: $\lambda = \lambda_4(x)$.

which does not coincide with the lowest eigenvalue of $\tilde{H}$. The reason is that here the quantity $\langle s|\psi_0\rangle$ in (14) diverges. This phase corresponds to large forward currents.

Phase B: $[(x < x_c) \wedge (\lambda_1 < \lambda < \lambda_2)] \vee [(x > x_c) \wedge (\lambda_1 < \lambda < \lambda_4)]$, where we defined x_c as

$$x_c = \frac{-\eta + (\beta+\gamma)^2 - \alpha\gamma + \beta\delta}{2\beta(\beta+\gamma)} \tag{47}$$

(see figure 4). In this region the spectrum of $\tilde{H}$ is gapped and $e(\lambda)$ coincides with the lowest eigenvalue:

$$e(\lambda) = \frac{\alpha\beta}{\beta+\gamma}(1-\mathrm{e}^{-\lambda}) + \frac{\gamma\delta}{\beta+\gamma}(1-\mathrm{e}^{\lambda}). \tag{48}$$

The quantities $\langle s|\psi_0\rangle$ and $\langle\psi_0|P_0\rangle$ are finite.

Phase C: $(x < x_c) \wedge (\lambda_2 < \lambda < \lambda_3)$ (see figure 4). In this phase the spectrum of $\tilde{H}$ is gapless. The scalar products $\langle s|\psi_0\rangle$ and $\langle\psi_0|P_0\rangle$ are finite (here $|\psi_0\rangle$, which is the ground-state of $\tilde{H}$, has to be understood as $|\psi_{k\to 0}\rangle$), consequently $e(\lambda)$ is given by the lowest eigenvalue:

$$e(\lambda) = \alpha + \beta + \gamma + \delta - 2\sqrt{(\alpha\mathrm{e}^{-\lambda} + \delta)\,(\beta + \gamma\mathrm{e}^{\lambda})} \tag{49}$$

Phase D: $[(x < x_c) \wedge (\lambda > \lambda_3)] \vee [(x > x_c) \wedge (\lambda > \lambda_4)]$ (see figure 4). In this phase the quantity $\langle\psi_0|P_0\rangle$ diverges and $e(\lambda)$ differs from the lowest eigenvalue of $\tilde{H}(\lambda)$:

$$e(\lambda) = \alpha + \beta + \gamma + \delta - \left(\beta + \gamma\mathrm{e}^{\lambda}\right) x - \frac{\alpha\mathrm{e}^{-\lambda} + \delta}{x}. \tag{50}$$

It is interesting that here the large deviation of current fluctuations retains a dependence on the initial state of the system.

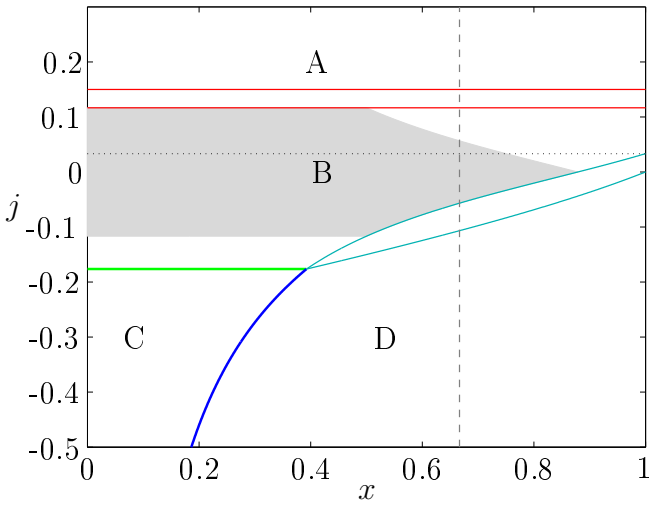

Figure 5. The x–j phase diagram for $\alpha = \gamma = \delta = 0.1$, $\beta = 0.2$. At first order transition lines (A–B and B–D) mixed phases appear. Red line: $j = j_a$ or $j = j_b$, green line: $j = j_c$, blue line: $j = j_d(x)$, cyan line: $j = j_e(x)$ or $j = j_f(x)$. The horizontal dotted line shows the mean current, the vertical dashed line indicates the the specific value of x which corresponds to the steady state initial condition.

For the physical interpretation of these phases it is better to consider $\hat{e}(j)$, which can be obtained from $e(\lambda)$ by a Legendre transformation. $\hat{e}(j)$ has the following forms in the different regions of figure 5:

$$\hat{e}(j) = \begin{cases} f_j(\alpha,\gamma) & \text{A} \\ f_j\left(\frac{\alpha\beta}{\beta+\gamma}, \frac{\gamma\delta}{\beta+\gamma}\right) & \text{B} \\ f_j(\alpha,\gamma) + f_j(\beta,\delta) & \text{C} \\ f_j(\alpha,\gamma) + \beta(1-x) + \delta\left(1-x^{-1}\right) + j\ln x & \text{D} \end{cases} \tag{51}$$

with

$$f_j(a,b) = a + b - \sqrt{j^2+4ab} + j\ln\frac{j+\sqrt{j^2+4ab}}{2a}. \tag{52}$$

We remark that $f_j(a,b)$ has a simple physical meaning. Consider a single particle performing a simple random walk on the infinite one-dimensional lattice with right (left) hopping rate a (b). Then the large deviation function of the distance travelled by this particle is given by $f_j(a,b)$.

In phase A only the rates for the first bond determine the large deviation function. For such large currents particles typically pile up on the site, which then acts as an infinite reservoir. In this case the behaviour of the two bonds decouples, so the current distribution across the input bond is entirely controlled by the two Poisson processes at rate α and γ. This explains the first line in (51). The fact that in these (very unlikely) realizations the occupation number increases with time, is consistent with the divergence of $\langle s|\psi_0\rangle$. In stochastic systems such divergence is usually associated with the lack of a steady state. Here, the model does have a steady state so that realizations involving piling-up of particles (condensation) are never observed in the infinite time

limit. However, as indicated, they characterize the fluctuations that can be observed over a large but finite measuring period t. We therefore use the term "instantanous condensate".

In phase B, which always contains the mean steady-state current ($\lambda = 0$), the four rates enter symmetrically in the large deviation function. Note that the combinations $\alpha\beta/(\beta+\gamma)$ and $\gamma\delta/(\beta+\gamma)$ are the effective renormalized hopping rates of two exclusion particles with left (right) hopping rates α (γ) and β (δ), in the case where they form a bound state [39]. In this regime the occupation of the site, which maps to the distance between the two exclusion particles, remains finite. The existence of this "two-particle bound state" is also manifested in the gapped spectrum of $\tilde{H}$.

Although the naive approach (i.e. identifying $e(\lambda)$ with the lowest eigenvalue of $\tilde{H}$) still works in phase C, the large deviation function takes a different form here. For these large negative currents (and small initial occupation) it is needed that the current across the other bond also takes a large negative value (unlike in phase A). It can be seen in (51) that the contribution of the two bonds factorize suggesting that they act independently. This can be traced back to the change in the spectrum which becomes gapless in this regime, corresponding to a two-particle unbound state. The distance between the two particles (or equivalently the occupation of the site) grows as the square-root of time in such realizations—again we refer to this temporary piling-up as instantaneous condensation.

Phase D is in some sense the counterpart of phase A. Typical realizations contributing to these exponentially small probabilities start at a very high occupation (initial condensate) which then decreases during the observation time. For fixed j, this is possible only for sufficiently large values of x. This initial singularity is indicated by the divergence of $\langle\psi_0|P_0\rangle$.

One can see in the x–j phase diagram (see figure 5) that in between phases A–B and B–D transition regions appear. These regimes correspond to a single transition line in the x–λ diagram along which the derivative of $e(\lambda)$ is discontinuous. This is entirely analogous to ordinary equilibrium phase transitions where different thermodynamical potentials are Legendre transforms of each other and in certain phase diagrams mixed regions (e.g. liquid–gas) appear at first order phase transitions lines. For the full analogy one can consider the following identifications: $j \rightarrow$(specific) volume; $\lambda \rightarrow$pressure; $\hat{e}(j) \rightarrow$ Helmholtz free energy (density); $e(\lambda) \rightarrow$ Gibbs free energy (density). One can immediately see that the analogue quantity of the system size N is the measurement time t in our model which must diverge if a true phase transition is to exist. In the mixed regions of the phase diagram the system segregates in time, i.e., for some finite fraction of the whole measurement time the system behaves as being on one boundary of the mixed phase while for the rest of the time it switches to the other boundary.§

§ Mathematically speaking, knowledge of $e(\lambda)$ is only sufficient to determine $\hat{e}(j)$ where $e(\lambda)$ is differentiable. If $e(\lambda)$ is non-differentiable then $\hat{e}(j)$ is, in general, non-convex; Legendre transform of the non-differentiable points in $e(\lambda)$ then yields straight-line sections of the convex envelope of $\hat{e}(j)$. However in our case, the physical argument based on phase separation in time, indicates that the linear

One can formally consider t as a space dimension. Then a path in the configuration space of the original model becomes a configuration of the new model, see e.g., [43]. If the original model has finite number of configurations then this leads to only one (diverging) dimension (t) in the new model hence no phase transition is possible in this case. Therefore for a real phase transition to take place one needs infinitely many possible configurations in the original model. In our single site model this is achieved in the simplest way.

The above analogy between ordinary equilibrium phase transitions and transitions in the large deviation function of current fluctuations suggests that the ordinary free energy can be considered as the large deviation function of density fluctuations, which is indeed the case. Vice versa, the large deviation of current fluctuations $\hat{e}(j)$ can be interpreted as some kind of "dynamical free energy". The main difference between the two cases is that the pressure can easily be controlled and measured in an experiment, whereas that is not the case with λ. So far it seems that the only way to make measurements for $e(\lambda)$ or $\hat{e}(j)$ is the highly inefficient method of measuring the probabilities of large current fluctuations in a system where $\lambda = 0$ (zero pressure). However in the next section, we will see that with the help of a neat trick λ becomes adjustable in computer simulations. Still, the question of the (experimental) physical interpretation of this parameter remains open.

4.2. Range of validity of GC symmetry

Armed with the detailed knowledge of the phase diagram for our single-site model, we now return to the original question of the validity of the fluctuation theorem. For the GC symmetry to hold for currents of magnitude j, we require that both j and $-j$ are in phases B or C (in which $e(\lambda)$ is given by the lowest eigenvalue of $\tilde{H}$). This immediately implies that the symmetry is seen only in the restricted interval $[-j_{\max}, j_{\max}]$ where

$$j_{\max} \equiv \min(j_b, -j_e). \tag{53}$$

This is shown as the shaded regime in figure 5. Note that $j_{\max}$ depends on the initial distribution and that the GC symmetry is not seen at all above some critical value of x.

Now let us investigate the ratio of probabilities for forward and backward currents outside the symmetry regime. For non-zero x, then one sees a crossover to

$$\begin{aligned} \hat{e}(-j) - \hat{e}(j) &= f_{-j}(\alpha,\gamma) + \beta(1-x) + \delta(1-x^{-1}) - j\ln x - f_j(\alpha,\gamma) \\ &= \beta(1-x) + \delta(1-x^{-1}) + j\ln\left(\frac{\alpha}{\gamma x}\right). \end{aligned} \tag{54}$$

In other words, for large j, the quantity $\hat{e}(-j) - \hat{e}(j)$ is linear with slope $\ln\left(\frac{\alpha}{\gamma x}\right)$. At first glance, this may appear to be the extended fluctuation theorem of section 2.6. However,

sections obtained via Legendre transform *do* yield the correct form for $\hat{e}(j)$ in the transition regimes (i.e., the large deviation function *is* still convex). For a mathematical account of the subtleties of large deviation theory the reader is referred to [40]; the application to statistical mechanics is discussed in [41, 42].

the slope of the linear section is not as predicted there—in particular, it is not zero for an initial steady-state distribution (i.e., the ratio of forward and backward currents does not saturate to a constant value). We emphasize also that $\hat{e}(j)$ itself does not become linear for large $|j|$ as it does in the case of boundary terms which are independent of the bulk contribution. It would be interesting to develop a general argument to predict the behaviour in cases, such as this, where correlations are important.

4.3. Generalizations

Although the calculations of appendix A and section 4.1 were for a single-site model with the rates $w_n = 1$ and a Boltzmann initial distribution (43) we argue here that they also have implications for more general single-site models.

Firstly, we note that results for the case $w_n = a$ where a is any finite positive constant are trivially given by rescaling $\beta \to a\beta$ and $\gamma \to a\gamma$. More generally, we argue that for the long-time behaviour only the large-n asymptotics of w_n are relevant and thus the results for any bounded w_n function $\lim_{n\to\infty} w_n = a$ are obtained by the same rescaling of β and γ. To see this note that the lowest eigenvalue in the gapped state (40) is independent of w_n and the condition for occurrence of instantaneous condensates (divergence of the scalar products) depends only on the behaviour for $n \to \infty$ as does the asymptotic current distribution out from such an instantaneous condensate. However the convergence to the long-time limiting behaviour is expected to depend on the form of w_n making direct comparison of finite-time simulation results difficult.

By a similar argument, we expect any initial distribution with the same large-n behaviour to lead to the same current large deviations. Since the elements of the lowest eigenvector $|\psi_0\rangle$ fall off exponentially with n, this means that any initial distribution with super-exponential decay should give the same result as the empty initial site (or any other fixed initial configuration), i.e., $x = 0$. Similarly, if the weight of configurations in the initial state decays slower than exponentially, then this corresponds to the case $x = 1$.

Finally, we remark that results for the current across the output bond can always be obtained by the replacements: $\alpha \leftrightarrow \delta$, $\beta \leftrightarrow \gamma$, $p \leftrightarrow q$, $\lambda \leftrightarrow -\lambda$, $j \leftrightarrow -j$, i.e., by left-right reflection. In section 6 we discuss extensions to larger systems.

5. Numerical results for $e(\lambda)$

In [1], the analytical prediction for $\hat{e}(j)$ was checked via direct Monte Carlo simulation. However, it is difficult to get high quality data for long-times since one is looking for exponentially unlikely events. In this section we demonstrate instead the application of a recent algorithm by Giardinà, Kurchan and Peliti [2] to calculate $e(\lambda)$ directly.

5.1. Cloning algorithm

The method is based on an alternative interpretation of (12). Here $\tilde{H}$ acts as the generator of some kind of time evolution. However, it cannot be an ordinary stochastic evolution operator since it does not satisfy the normalization condition (8), therefore it does not conserve probability. The idea is to consider an ensemble of N identical systems (clones), where the number of "individuals" being in the same configuration σ is denoted by P_σ. Here the size N of the "population" can vary in time, which means that there is no conservation law for the vector $|P\rangle$ as it is not a probability vector anymore ($\langle s|P\rangle \neq 1$). The off-diagonal elements of $\tilde{H}$ give the currents from one configuration to another. The fact that $\tilde{H}$ is not normalized means that the sum of the currents from a specific configuration into any other is not necessarily equal to the loss in that configuration. This means that individuals can reproduce (i.e. introduce another copy of the system prepared in the same configuration as the ancestor by increasing N by one) or die at given rates, where this rate depends on the configuration σ, and is given by $\sum_{\sigma'} \tilde{H}_{\sigma'\sigma}$.

The process described above can easily be simulated by Monte Carlo methods. The quantity to measure is the average rate of growth of the whole population for large times, which directly gives $e(\lambda)$. In practice however, one chooses a sufficiently large N which is kept constant by renormalizing the size of the population after each "birth" or "death" (while keeping a record of growth). The method was originally introduced for discrete-time update (for details see [2]) but is straightforwardly modified to the continuous time case (see also [44]).

Note that $\tilde{H}$ does not give the full probabilistic description of the above-defined stochastic cloning process. The deterministic time evolution (often called rate equation) given by $\tilde{H}$ refers only to the averages in a large population ($N \to \infty$). Therefore, in order to obtain reliable results one has to reduce the possible fluctuations of the (cloning) process by choosing large N.

In a modified version of the algorithm the mean (integrated) current is measured instead of the growth rate. This gives the derivative of $e(\lambda)$, which can be then numerically integrated (with the fixed condition $e(0) = 0$). We note that, in this algorithm, descendants of a given clone inherit not only the configuration of the parent but also the actual value of the parent's integrated current. The advantage of this modified algorithm is that it gives less noise.

5.2. Results for the one-site ZRP with empty initial condition

We performed the above programme for the one-site ZRP. Since $e(\lambda)$ is known exactly, this should be considered as a test of the cloning method. Results are shown in figure 6(a) for the case of an empty initial site. It can be seen that the resulting data points for $N = 10^3$ and $t = 10^3$ lie very close to the exact ($t = \infty$) results in phases A and B. However, in phase C there is a significant deviation and the difference decreases with increasing N. A systematic analysis of the N-dependence of the cloning method is still

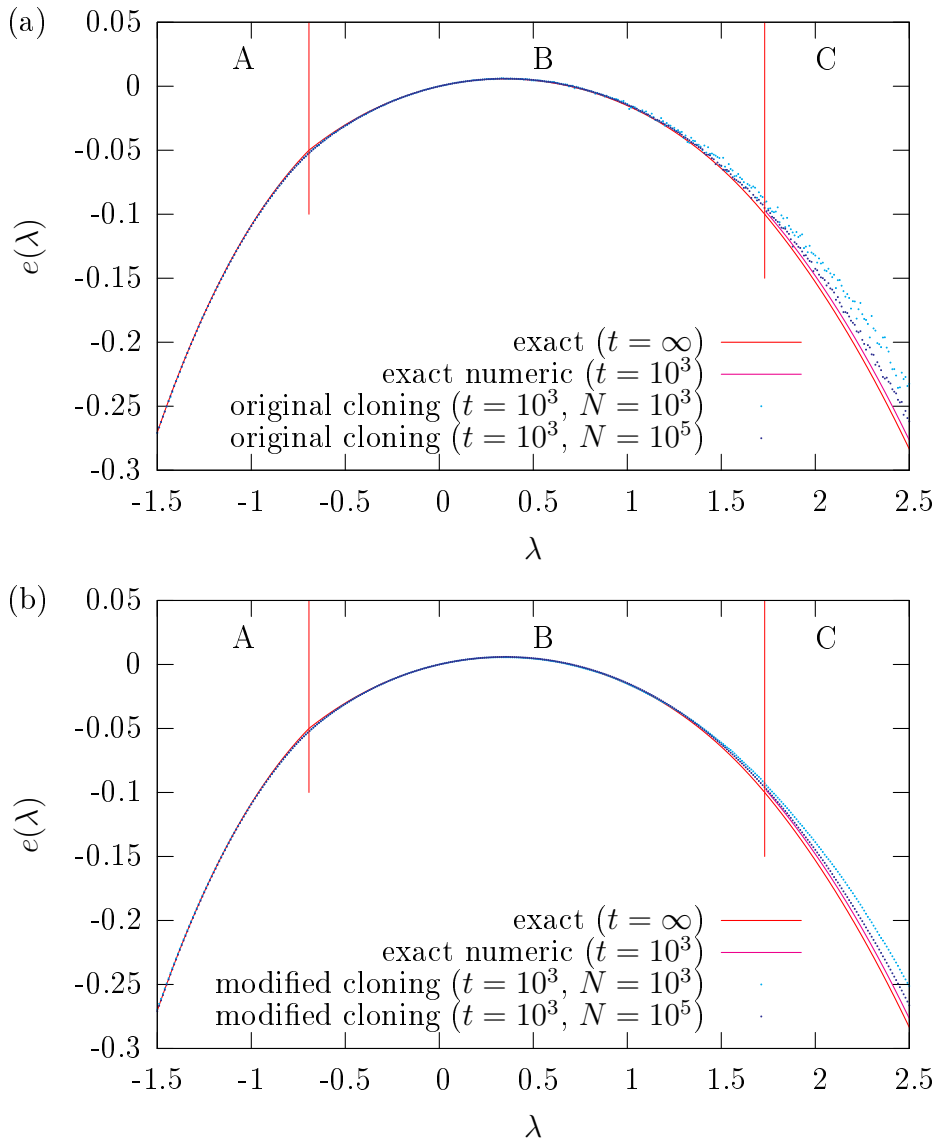

Figure 6. Cloning simulation results for the one-site ZRP with empty initial condition compared to the exact analytical results. The plots show the result of two versions of the algorithm, both with two different values of N. The original cloning algorithm (a) produces more noise in the gapless regime than a variant of it (b) whereby the derivative of the function $e(\lambda)$ is measured and then numerically integrated to get $e(\lambda)$. In the gapless case the convergence in N is slow. For reasonable values of N there is a systematic deviation (overestimation) from the exact result. Parameters: $\alpha = \gamma = \delta = 0.1$, $\beta = 0.2$.

lacking so it is not obvious how to set the value of N in general to provide a good balance between accuracy and simulation speed.

Our numerical results suggest that in the gapless phase the simulation could be very sensitive to the value of N and could deliver unreliable results for the accessible range. We believe that this limitation of the cloning method is related to the gapless

spectrum and would not show up in cases where the state space is finite.

Figure 6(b) shows the results of a modified cloning algorithm, where the derivative of $e(\lambda)$ was measured directly and then numerically integrated. Despite the smoother results the same type of discrepancy shows up in this version of the simulation.

In the stationary state of the cloning process (if it exists), the distribution of the occupation number of clones is expected to follow the ground-state of $\tilde{H}$. We measured this distribution in a representative point of phase B ($\lambda = 1.0$, $x = 0$) and C ($\lambda = 2.2$, $x = 0$). Results are shown in figure 7-8. The measured distribution in phase B follows the one suggested by the theory. In phase C (gapless phase) however, there is a significant difference between the theory and the measurement. This suggests that in the gapless phase the algorithm fails to find the true ground-state, hence $e(\lambda)$ is systematically overestimated in the measurement. This is consistent with the results shown in figure 6. We note that in phases A and D there is no steady state of the cloning process.

As discussed above, the cloning method strongly relies on the assumption that the number of clones is infinite. It is highly non-trivial to determine what type of correction appears if N is finite (as in computer simulations). Our numerical results show that this correction is much higher in the gapless phase. This is possibly due to the fact that with a finite number of clones one cannot recover the exact distribution but some fluctuations are introduced. In the case of a gapped spectrum the system has a strong tendency to the ground state, therefore these fluctuations are suppressed and do not play a crutial role as long as they are sufficiently small (N is sufficiently large). In the gapless case however, the relaxation to the true ground-state becomes slow and therefore, due to the fluctuations, states other than the ground state are also represented in the sample with a non-negligible weight (see figures 7-8).

It is also possible to define $e(\lambda)$ for finite time, which we denote by $e(\lambda)_t$.

$$e(\lambda)_t = -\frac{1}{t}\ln\langle \mathrm{e}^{-\lambda J}\rangle \tag{55}$$

Since measurements can be made only for finite times, the corrections to $e(\lambda)$ are of great interest. It is relatively easy to calculate the finite-time corrections in the single-site model based on (A.13). In phases A-B-D the leading contribution comes from a pole which leads to an $\mathcal{O}(1/t)$ correction in $e(\lambda)_t$. In the gapless phase C the leading contribution is given by the saddle point integration. Since the first order term vanishes here the dominant contribution gives $\mathcal{O}(t^{-2/3}\exp(-e(\lambda)t))$ in (A.13), which leads to a $(2/3)\ln(Ct)/t$ correction, where C is some constant. We performed exact numeric calculations of $e(\lambda)_t$ by evaluating the integrals in (A.13) and this is in good agreement with our analytical findings. For details see figure 9.

5.3. Non-empty initial condition

It is, in principle, possible to start the system from any initial condition in the cloning algorithm. Ideally, one would hope that the method reproduces the exact results in this regime. However, since the number of clones is finite, the initial distribution has always

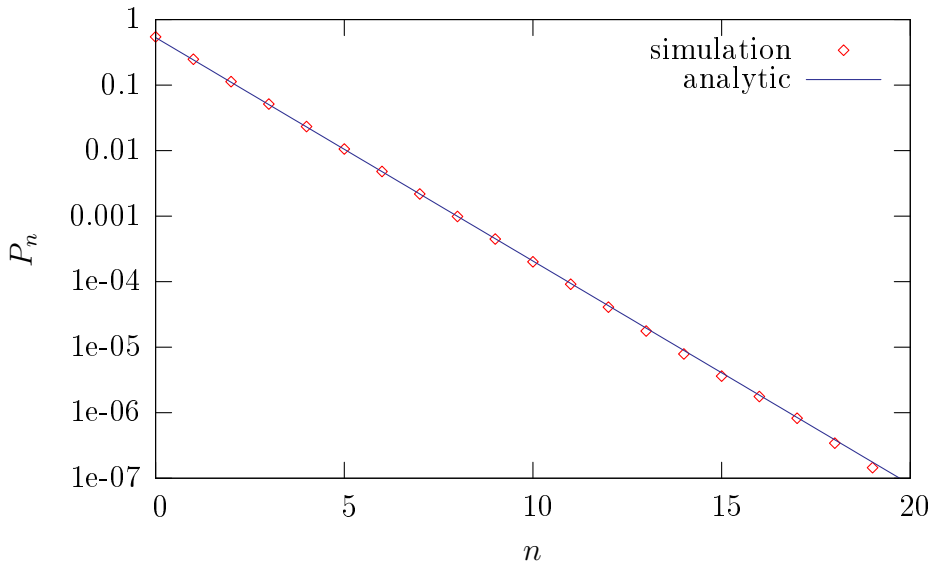

Figure 7. Distribution of the occupation number in the "steady state" of the cloning algorithm at $\lambda = 1.0$ (phase B) compared to the analytical results (ground-state of $\tilde{H}$). Parameters: $\alpha = \gamma = \delta = 0.1$, $\beta = 0.2$, $t = 10000$, $N = 10^5$.

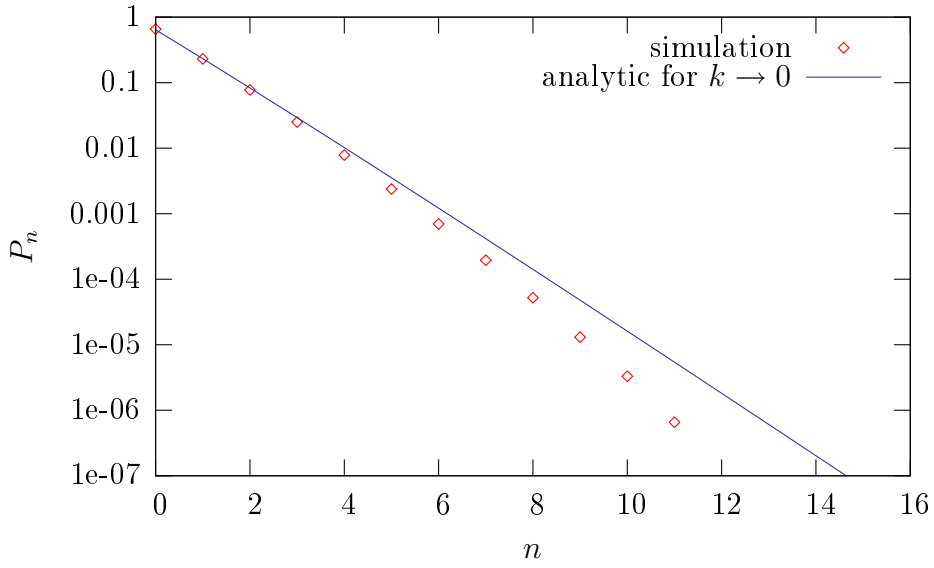

Figure 8. Distribution of the occupation number in the "steady state" of the cloning algorithm at $\lambda = 2.2$ (phase C) compared to the analytical results. Taking the limit of expression (A.3) at $k \to 0$ together with (A.7) one obtains $\langle n|\psi_{k\to 0}\rangle \sim \phi^{-n}(n + y/(y-1))$. The algorithm seems to fail in this gapless region and the distribution does not converge to the ground-state of $\tilde{H}(\lambda)$. Parameters: $\alpha = \gamma = \delta = 0.1$, $\beta = 0.2$, $t = 10000$, $N = 10^5$.

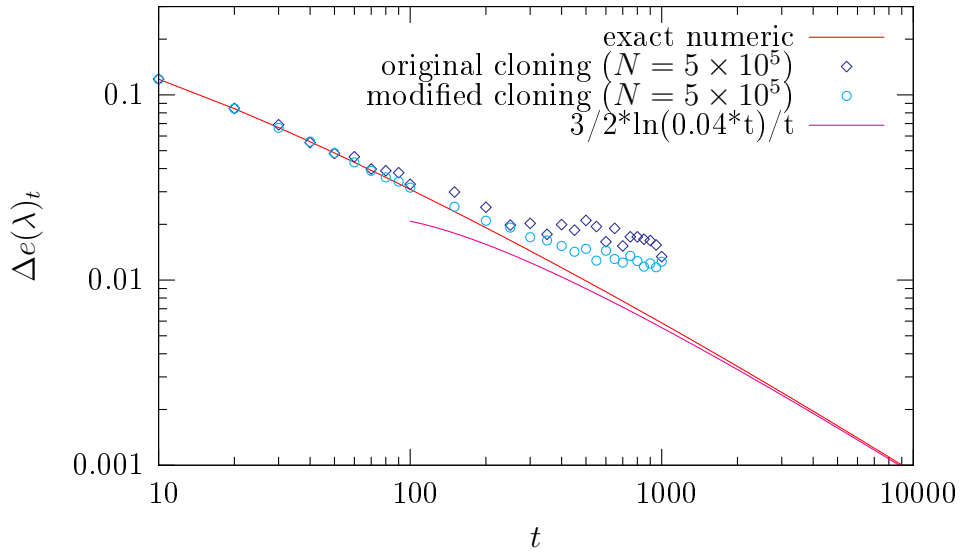

Figure 9. Plotted is the finite-time correction $\Delta e(\lambda)_t = e(\lambda)_t - e(\lambda)$ against t in the gapless phase at $\lambda = 2.2$. Exact numerical calculations are compared to the simulation results. The cloning method (with fixed N) becomes unreliable for large t. Parameters: $\alpha = \gamma = \delta = 0.1$, $\beta = 0.2$.

a finite (although arbitrarily large) cutoff. Although this is a minor change in the initial distribution, it becomes crucially important when measuring large deviations. A long time measurement for an initial distribution with a finite cutoff gives the same results as for an initially empty lattice. For an initial distribution with exponential tails (the case that we consider) one would need $N \sim \exp(t)$ number of clones in a measurement of length t. This is practically unreachable for reasonably large t. For this reason it is not surprising that the algorithm breaks down in the initial-state-dependent phase.

6. Larger systems

In this section we extend our discussion to larger systems in order to demonstrate the generality of the fluctuation theorem breakdown for the current fluctuations. We consider the L-site zero-range process with parameters as defined in section 3 and take again $w_n = 1$ (but expect qualitatively the same results for any bounded w_n). For definiteness we assume that the boundary parameters have been chosen to give a well-defined steady state with mean ("forward") current to the right. Once again, we focus on the behaviour of current fluctuations across the input ("0th") bond but indicate also how to extend our approach to treat the fluctuations across bulk bonds. In section 6.1, we first outline our general method, in particular the use of a powerful mapping to effective one-site systems. This leads to a statement about the regime of validity of the GC symmetry (section 6.2) and some comments on generalizations (section 6.3). Finally, in section 6.4, we give explicit results for a two-site system and make comparisons with

numerical data.

6.1. General approach

We remind the reader that, for a ZRP of arbitrary size, one can rigorously calculate the lowest eigenvalue ϵ_0 *in the gapped phase* of the modified Hamiltonian measuring the input current together with the associated left and right eigenvectors $\langle\psi_0|$ and $|\psi_0\rangle$. Details of the calculations are given in [36], pertinent results are summarized in section 3 above. In order to determine the limit of the GC symmetry one has to ascertain the values of λ at which the scalar products $\langle s|\psi_0\rangle$ and $\langle\psi_0|P_0\rangle$ diverge whilst keeping in mind that the divergence of the normalization of the gapped eigenvalue $\langle\psi_0|\psi_0\rangle$ indicates the cross-over to a gapless regime. To determine the behaviour of current fluctuations when these scalar products diverge we can appeal to the heuristic argument based on instantaneous condensates.

This process is considerably simplified by relating the current fluctuations in an L-site system to those in a one-site system with effective parameters. We note that with the definitions

$$\alpha_l = \frac{\alpha(p/q)^{l-1}(p-q)}{(p-q+\gamma)(p/q)^{l-1}-\gamma} \tag{56}$$

$$\beta_l = \frac{\beta(p/q)^{L-l}(p-q)}{p-q-\beta+\beta(p/q)^{L-l}} \tag{57}$$

$$\gamma_l = \frac{\gamma(p-q)}{(p-q+\gamma)(p/q)^{l-1}-\gamma} \tag{58}$$

$$\delta_l = \frac{\delta(p-q)}{p-q-\beta+\beta(p/q)^{L-l}}, \tag{59}$$

the lowest eigenvalue (40) in the gapped phase of the modified Hamiltonian for an L-site system (39) can be written in the form

$$\epsilon_0 = \frac{\alpha_l\beta_l}{\beta_l+\gamma_l}(1-\mathrm{e}^{-\lambda}) + \frac{\gamma_l\delta_l}{\beta_l+\gamma_l}(1-\mathrm{e}^{\lambda}), \tag{60}$$

and the corresponding left and right eigenvectors are defined by fugacities

$$z_l = \frac{\alpha_l\mathrm{e}^{-\lambda}+\delta_l}{\beta_l+\gamma_l} \tag{61}$$

$$\tilde{z}_l = \frac{\beta_l+\gamma_l\mathrm{e}^{\lambda}}{\beta_l+\gamma_l}. \tag{62}$$

In other words, the one-site marginal for site l and the eigenvalue have exactly the same form as in the one site problem with effective α_l and γ_l (β_l and δ_l) determined by all the rates to the left (right) of l. This fact relies on the product-state character of the lowest eigenvector of the modified Hamiltonian corresponding to the current being measured. Notice that, by construction, $\alpha_1=\alpha$, $\gamma_L=\gamma$, $\beta_L=\beta$ and $\delta_L=\delta$. We also remark that the parameter combinations $\alpha_l\beta_l/(\beta_l+\gamma_l)$ and $\gamma_l\delta_l/(\beta_l+\gamma_l)$ are independent of l and are

equal to the left/right hopping rates of an N particle bound state in the corresponding exclusion process. Equivalently, in current space we have

$$\hat{e}(j) = f_j\left(\frac{\alpha_l\beta_l}{\beta_l+\gamma_l}, \frac{\gamma_l\delta_l}{\beta_l+\gamma_l}\right). \tag{63}$$

This important observation allows us to utilize the exact results already obtained for the one-site case to build up the phase diagram for an L-site system.‖

Recall that $\lambda = 0$ corresponds to the mean current. The asymptotic probability of seeing a current fluctuation larger than the mean is given by the behaviour of $e(\lambda)$ for λ negative. To determine the $\lambda < 0$ part of the phase diagram we carry out the following procedure:

(i) Start with $\lambda = 0$ and $e(\lambda)$ given by ϵ_0 of (60).

(ii) Decrease λ until $\langle s|\psi_0\rangle$ diverges on one of the sites, which we label l_1. From the one-site picture we immediately see that this will happen at

$$\lambda_1(l_1) \equiv \lambda_1(\alpha_{l_1}, \beta_{l_1}, \gamma_{l_1}, \delta_{l_1}) \tag{64}$$

with λ_1 defined as in Table 1. Physically, we argue (just as in the single-site case) that this divergence corresponds to the "piling-up" of particles on site l_1. For $\lambda < \lambda_1(l_1)$ the current fluctuations (across the input bond) only depend on the part of the system to the left of site l_1 and we thus expect a crossover to

$$e(\lambda) = \alpha_{l_1}(1-\mathrm{e}^{-\lambda}) + \gamma_{l_1}(1-\mathrm{e}^{\lambda}), \tag{65}$$

which corresponds to a current large deviation function.

$$\hat{e}(j) = f_j(\alpha_{l_1}, \gamma_{l_1}). \tag{66}$$

Just as in the single-site case, $e_0(\lambda)$ is continuous but not differentiable at $\lambda_1(l_1)$ so the two phases in current space are separated by a linear transition regime whose explicit form is simply obtained from the effective single-site picture.

(iii) Now, with such an "instantaneous condensate" on site l_1, the left-hand part of the system looks just like a system of size $l_1 - 1$ with right-hand boundary rates p and q. We can then write down the new ground state $|\psi_0\rangle$ in terms of redefined effective parameters α_l, β_l, γ_l and δ_l.

(iv) Repeat steps (ii) and (iii) recursively until...

(v) At some value of λ, $\langle s|\psi_0\rangle$ (with $|\psi_0\rangle$ a function of the effective parameters) diverges on site 1 and the large deviation function takes the form

$$e(\lambda) = \alpha(1-\mathrm{e}^{-\lambda}) + \gamma(1-\mathrm{e}^{\lambda}) \tag{67}$$

$$\hat{e}(j) = f_j(\alpha, \gamma). \tag{68}$$

(again with a linear transition regime in j-space). In other words, for very large forward currents, only the hopping parameters across the input bond are significant.

‖ Although our results can be applied to large systems by taking the thermodynamic limit $L \to \infty$, this limit does not necessarily commute with the long-time limit $t \to \infty$. Our analysis therefore does not address the form of current fluctuations in a genuinely infinite system (taking the limit $L \to \infty$ first, followed by $t \to \infty$).

In a similar fashion one can investigate what happens for currents smaller than the mean by increasing λ from zero. For simplicity, let us first take a fixed initial configuration so that $\langle\psi_0|P_0\rangle$ is always finite. At $\lambda_2(l) \equiv \lambda_2(\alpha_l, \beta_l, \gamma_l, \delta_l)$, $\langle\psi_0|\psi_0\rangle$ diverges on site l, corresponding to a transition to a gapless phase. The minimum value of $\lambda_2(l)$ occurs at some l_2 (which depends on the parameters of the model) so we first see a crossover to

$$e(\lambda) = \alpha_{l_2} + \beta_{l_2} + \gamma_{l_2} + \delta_{l_2} - 2\sqrt{(\alpha_{l_2}\mathrm{e}^{-\lambda} + \delta_{l_2})(\beta_{l_2} + \gamma_{l_2}\mathrm{e}^{\lambda})} \tag{69}$$

$$\hat{e}(j) = f_j(\alpha_{l_2}, \gamma_{l_2}) + f_j(\beta_{l_2}, \delta_{l_2}). \tag{70}$$

In other words, to sustain a large backwards current we have an instantaneous condensate on site l_2 and the product of current distributions across the two independent parts of the system. For increasing backwards currents, one can then repeat the procedure for the two subsystems (each with redefined effective parameters), increasing λ and looking for the next site where $\langle\psi_0|\psi_0\rangle$ diverges. Eventually, for very large backward currents we expect instantaneous condensates on all sites and a current large deviation function given by

$$\hat{e}(j) = f_j(\alpha, \gamma) + (L-1)f_j(p, q) + f_j(\beta, \delta) \tag{71}$$

For a distribution over initial configurations, the situation is more complicated but again we can make progress based on the effective one-site picture. For an initial particle distribution which is a product measure of Boltzmann distributions with site dependent fugacity x_l, then $\langle\psi_0|P_0\rangle$ will diverge on the lth site at $\lambda_4(l) \equiv \lambda_4(\alpha_l, \beta_l, \gamma_l, \delta_l, x_l)$ leading to a crossover to an initial-state dependent regime. If l_4 is the (initial-condition-dependent) value of l corresponding to the minimum of $\lambda_4(l)$ then, for large initial fugacities we expect to find first a transition to

$$e(\lambda) = \alpha_{l_4} + \beta_{l_4} + \gamma_{l_4} + \delta_{l_4} - (\beta_{l_4} + \gamma_{l_4}\mathrm{e}^{\lambda})x_{l_4} - (\alpha_{l_4}\mathrm{e}^{-\lambda} + \delta_{l_4})x_{l_4}^{-1} \tag{72}$$

$$\hat{e}(j) = f_j(\alpha_{l_4}, \gamma_{l_4}) + \beta_{l_4}(1 - x_{l_4}) + \delta_{l_4}(1 - x_{l_4}^{-1}) + j \ln x_{l_4}. \tag{73}$$

Once again, we see a factorization of the asymptotic current distribution across the two sub-systems to the left and right of l_4. In principal, one can try to build up the complete phase diagram by next checking for the divergence of $\langle\psi_0|P_0\rangle$ on other sites as λ is further increased. Another scenario, for small initial fugacities, involves first a transition to a gapless phase and then a transition to the initial condition dependent phase when $\lambda = \lambda_3(l)$ as a function of the redefined effective rates.

6.2. Range of validity of GC symmetry

The effective one-site picture provides an elegant way to summarize the range of validity for the GC symmetry in ZRPs of arbitrary size. By comparison with (53) and with the shaded regime in figure 5, we see that, for given initial fugacities $\{x\}$, the symmetry relation for input current will only be obeyed in the following current range:

$$|j| \leq \min(j_b(\alpha_{l_1}, \beta_{l_1}, \gamma_{l_1}, \delta_{l_1}), -j_e(\alpha_{l_4}, \beta_{l_4}, \gamma_{l_4}, \delta_{l_4}, x_{l_4})) \tag{74}$$

where l_i is the value of l at which $|\lambda_i(l)|$ takes its minimum value as a function of the effective rates given in (56)–(59). In the case where j_e is positive for some l then the symmetry will not be observed at all.

6.3. Further generalizations

We remark that the same condition as (74) should also apply for ZRPs with quenched disorder (i.e., with p and q bond dependent)—one needs only to determine the appropriate form for the effective rates. Indeed, building on the recent determination of the stationary state for such systems [45], we can show that the relevant parameter combinations are

$$\alpha_l = \frac{\prod_{i=0}^{l-1} \frac{p_i}{q_i}}{\sum_{i=0}^{l-1} \frac{1}{q_{l-i-1}} \prod_{k=1}^{i} \frac{p_{l-k}}{q_{l-k}}} \tag{75}$$

$$\beta_l = \frac{1}{\sum_{i=0}^{L-l} \frac{1}{p_{l+i}} \prod_{k=0}^{i-1} \frac{q_{l+k}}{p_{l+k}}} \tag{76}$$

$$\gamma_l = \frac{1}{\sum_{i=0}^{l-1} \frac{1}{q_{l-i-1}} \prod_{k=1}^{i} \frac{p_{l-k}}{q_{l-k}}} \tag{77}$$

$$\delta_l = \frac{\prod_{i=0}^{L-l} \frac{q_{l+i}}{p_{l+i}}}{\sum_{i=0}^{L-l} \frac{1}{p_{l+i}} \prod_{k=0}^{i-1} \frac{q_{l+k}}{p_{l+k}}} \tag{78}$$

where p_l (q_l) is the right (left) hopping rate across bond l and by definition $p_0 = \alpha$, $q_0 = \gamma$, $p_L = \beta$ and $q_L = \delta$. One can state (75-78) alternatively as a simple recursion relation:

$$\alpha_{l+1} = \frac{\alpha_l p_l}{\gamma_l + p_l} \tag{79}$$

$$\beta_{l-1} = \frac{\beta_l p_{l-1}}{\beta_l + q_{l-1}} \tag{80}$$

$$\gamma_{l+1} = \frac{\gamma_l q_l}{\gamma_l + p_l} \tag{81}$$

$$\delta_{l-1} = \frac{\delta_l q_{l-1}}{\beta_l + q_{l-1}} \tag{82}$$

Not surprisingly, these are again the renormalized two-particle hopping rates.

We conclude this subsection by indicating how to extend our approach to treat the current fluctuations across other bonds. In this case, the effective parameters are unchanged, but in all sites to the left of the bond in question the fugacities (61) and (62) must be replaced by

$$z_l = \frac{\alpha_l + \delta_l \mathrm{e}^{\lambda}}{\beta_l + \gamma_l} \tag{83}$$

$$\tilde{z}_l = \frac{\beta_l + \gamma_l \mathrm{e}^{-\lambda}}{\beta_l + \gamma_l}. \tag{84}$$

corresponding to the expressions for the *output* bond of a single-site system.

6.4. Example: Two-site system

In principle, the general approach outlined above can be used to determine the behaviour of current fluctuations in ZRPs of arbitrary size. However the implementation rapidly becomes tedious and the phase diagram complicated. Here, as a simple test case, we present results for a two-site system with empty initial condition ($x_l = 0$ for all l).

It is obvious that for any choice of parameters obeying $\alpha - \gamma < p - q < \beta - \delta$, the system has a well-defined steady state (i.e., no boundary condensation). One also gets a stationary state if the conditions

$$\alpha - \gamma < \beta - \delta < p - q \tag{85}$$

and

$$\frac{\alpha p}{p+\gamma} - \frac{\gamma q}{p+\gamma} < \beta - \gamma \tag{86}$$

are obeyed. These inequalities can easily be understood in the exclusion picture where the first two particles form a bound state with hopping rates $\frac{\alpha p}{p+\gamma}$ and $\frac{\gamma q}{p+\gamma}$. The condition for the bound state of this and the remaining single particle is just (86).

For definiteness, in the remainder of the discussion we assume that the rates obey (85) and (86). In this case, as λ is decreased from 0, $\langle s|\psi_0\rangle$ diverges first on site 2 (i.e., $l_1 = 2$). Similarly, as λ is increased from 0, $\langle \psi_0|\psi_0\rangle$ also diverges first on site 2 (i.e., $l_2 = 2$). Appealing to the heuristic "instantaneous condensates" picture we then obtain the following different regimes for the current large deviation function.

$$\hat{e}(j) = \begin{cases} f_j(\alpha,\gamma) & \text{A2} \\ f_j\Big(\frac{\alpha p}{p+\gamma}, \frac{\gamma q}{p+\gamma}\Big) & \text{A1} \\ f_j\Big(\frac{\alpha\beta p}{\gamma q+\beta p+\beta\gamma}, \frac{\gamma\delta q}{\gamma q+\beta p+\beta\gamma}\Big) & \text{B} \\ f_j\Big(\frac{\alpha p}{p+\gamma}, \frac{\gamma q}{p+\gamma}\Big) + f_j(\beta,\delta) & \text{C1} \\ f_j(\alpha,\gamma) + f_j(p,q) + f_j(\beta,\delta) & \text{C2} \end{cases}, \tag{87}$$

with

$$\begin{aligned} \text{A2}: &\quad j_a(\alpha,p,\gamma,q) < j \\ \text{A1}: &\quad j_a\left(\tfrac{\alpha p}{p+\gamma}, \beta, \tfrac{\gamma q}{p+\gamma}, \delta\right) < j < j_b(\alpha,p,\gamma,q) \\ \text{B}: &\quad j_c\left(\tfrac{\alpha p}{p+\gamma}, \beta, \tfrac{\gamma q}{p+\gamma}, \delta\right) < j < j_b\left(\tfrac{\alpha p}{p+\gamma}, \beta, \tfrac{\gamma q}{p+\gamma}, \delta\right) . \\ \text{C1}: &\quad j_c(\alpha,p,\gamma,q) < j < j_c\left(\tfrac{\alpha p}{p+\gamma}, \beta, \tfrac{\gamma q}{p+\gamma}, \delta\right) \\ \text{C2}: &\quad j > j_c(\alpha,p,\gamma,q) \end{aligned} \tag{88}$$

Here the currents j_a, j_b and j_c are as defined in Table 1; we label the phases in analogy to A, B and C in the single-site case and note that there are intermediate transition regions at the A2–A1 and A1–B crossovers. From the argument in 6.2 it is clear that the Gallavotti-Cohen symmetry should hold for small currents $j < j_b\left(\frac{\alpha p}{p+\gamma}, \beta, \frac{\gamma q}{p+\gamma}, \delta,\right)$.

Finally, we compare the Legendre transform of (87) with results for $e(\lambda)$ obtained via the cloning algorithm (see section 5). As shown in figure 10, we find excellent agreement except for $\lambda > \lambda_2\left(\frac{\alpha p}{p+\gamma}, \beta, \frac{\gamma q}{p+\gamma}, \delta\right)$ where $e(\lambda)$ is given by the lowest eigenvalue of a gapless spectrum. Just as in the single-site case we attribute this to limitations imposed by the finite number of clones.

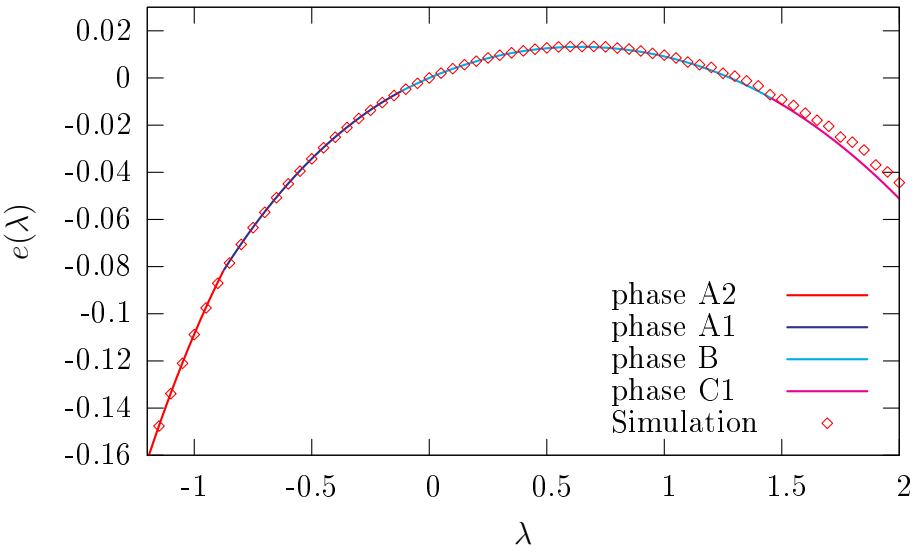

Figure 10. Cloning simulation results for two-site ZRP with empty initial condition compared with exact analytical results. Agreement is excellent except in the gapless phase. Parameters: $\alpha = \gamma = \delta = q = 0.1$, $\beta = 0.15$, $p = 0.24$, $t = 5000$, $N = 10^4$.

7. Summary

This paper focuses on the Gallavotti-Cohen (GC) fluctuation symmetry in the context of continuous-time Markov processes. In particular, it offers a contribution towards understanding the potential breakdown of this symmetry in systems with *infinite state space*. To set the scene for this, we first discussed how the symmetry is manifested for the large deviation function of currents in systems with *finite state space*. Our proof was based on that of Lebowitz and Spohn [11] (or Derrida et al. [46]) but slightly extends their work by considering more general currents. In the notational framework of this paper, the action functional of Lebowitz and Spohn can be obtained by choosing $\Theta_{\sigma,\sigma'} = \ln(w_{\sigma',\sigma}/w_{\sigma,\sigma'})$ and the GC symmetry then holds for J with $E = 1$. In this case, as shown in [11], J can be interpreted as an entropy current.

The above-mentionned proof of the fluctuation relation holds only for systems with finite state space—in systems with infinite state space the GC symmetry can be broken¶. In the spirit of van Zon and Cohen's earlier work for Langevin systems [23, 17], we next recapitulated the ideas leading to an "extended fluctuation theorem" in which (for stationary initial state) the ratio of probabilities of given forward (j) and backward ($-j$) currents approaches a constant for large values of j. We argued that this particular form of breakdown relies on the independence of bulk and boundary contributions to the current. The central aim of this paper was to study analytically a simple model where this condition is not met—the partially asymmetric Zero Range Process (ZRP)

¶ We remark that an infinite state space is *not* a sufficient condition for a breakdown of the Fluctuation Theorem. A counterexample is the ZRP with unbounded w_n as explained in section 3.2

on an open lattice [35, 36].

Specifically, we expanded on earlier results in [1], and showed in detail how to calculate the large deviations of the average particle current j in the one-site ZRP. The phase behaviour of the large deviation function can be physically understood by considering the possibility for an arbitrarily large number of particles to pile-up on the site ("instantaneous condensation"). Even in this single-site case, the phase diagram (parametrized by the time-averaged current and the initial state) shows a complex picture with first and second order phase transitions. These transitions are analogous to ordinary equilibrium phase transitions since formally the current large deviation function can be considered as a kind of dynamical free energy functional. In general, the GC symmetry holds only in a restricted interval $[-j_{\max}, j_{\max}]$, where $j_{\max}$ depends on the initial state. The relevant parameter of the initial state, which is denoted by x, can be considered as a kind of initial temperature. For large values of x the regime of validity of the fluctuation relation shrinks ($j_{\max}$ decreases) and reaches zero at a finite x. According to the above interpretation, this means that above a critical initial temperature the fluctuation theorem does not hold, even for small currents.

Although the one-site ZRP might be thought to be oversimplified, it is very instructive and already exhibits most features of the multiple-site version, which we have also studied in detail. In particular, we developed a heuristic argument based on mapping to an effective one-site system and considering the appearance of instantaneous condensates. The phase diagram can, in principle, be derived for any number of sites but it becomes increasingly complicated. As an example we showed how the current large deviation function can be obtained for a two-site ZRP. Again the phenomenon of instantaneous condensation is the physical mechanism leading to a breakdown of the GC fluctuation theorem.

Outside the symmetry regime, we found that the behaviour is somewhat different to that predicted by the extended fluctuation theorem of van Zon and Cohen, presumably due to the correlations (between bulk and boundary terms) in our model. There are evidently still open questions relating to the characterization of the fluctuation behaviour of different systems beyond the limits of Gallavotti-Cohen symmetry. For example, in another recent work [47] it was shown that the distribution of work fluctuations for a Brownian particle with Lévy noise (i.e., infinite variance) do not even have a large deviation form. It might be interesting to look for analogues of the resulting "anomalous fluctuation theorem" in the present framework of many-particle dynamics described by a master equation.

Our analytical results also made it possible to test the recently proposed cloning algorithm [2] that measures the Legendre transform of the large deviation function directly. The strength of this method is its efficiency and relative simplicity. The algorithm reproduces our analytical results in several phases. However, there are notable deviations in a phase where the spectrum of $\tilde{H}$, the effective Hamiltonian governing the current fluctuations, becomes gapless. Another weakness of the algorithm is that it is unable to capture the initial-state-dependence of the fluctuations. It is only the case

of a fixed initial configuration that this method can safely be used. These observations call for the development of a novel numerical algorithm which would not break down in cases where the cloning method does. One possibility here would be to develop a transition path sampling method.

Acknowledgments

This work was initiated while R. J. H. was working at the Forschungsentrum Jülich; we are very grateful to Gunter Schütz for many helpful discussions. It is also a pleasure to thank Jorge Kurchan, Vivien Lecomte and Julien Tailleur for advice about the implementation of the numerical algorithm. A. R. acknowledges financial support from the Hungarian Scientific Research Fund (Grant No. OTKA T-043734).

Appendix

A. Analytical calculations for single site model

A.1. Spectrum

Naively, one expects that the large deviation of current fluctuations is given by the lowest eigenvalue of $\tilde{H}$ according to (12). For this reason, we here study the spectrum of (44). First we transform $\tilde{H}$ into the symmetric form

$$\tilde{H}'(\lambda) = \Phi H(\lambda) \Phi^{-1} \tag{A.1}$$

using the diagonal operator

$$\Phi = \begin{pmatrix} \phi & 0 & 0 & \cdots \\ 0 & \phi^2 & 0 & \cdots \\ 0 & 0 & \phi^3 & \cdots \\ \vdots & \vdots & \vdots & \ddots \end{pmatrix}, \quad \text{with } \phi = \sqrt{\frac{\gamma \mathrm{e}^{\lambda} + \beta}{\alpha \mathrm{e}^{-\lambda} + \delta}}. \tag{A.2}$$

The diagonalization of $\tilde{H}'(\lambda)$ is easily done by a Fourier transformation. We introduce $y(\lambda) = \sqrt{(\gamma \mathrm{e}^{\lambda} + \beta)(\alpha \mathrm{e}^{-\lambda} + \delta)} / (\beta + \gamma)$ which determines the character of the spectrum as follows:

$y(\lambda) > 1$ Here the spectrum is entirely continuous. The eigenvector $|\psi'(k)\rangle$ corresponding to wave number $k \in (0, \pi]$ takes the form

$$|\psi'(k)\rangle = \sqrt{\frac{2}{\pi}} \sum_{n=0}^{\infty} \sin(kn + \varphi) |n\rangle, \quad \text{with } \mathrm{e}^{2i\varphi} = \frac{y(\lambda)\mathrm{e}^{ik} - 1}{y(\lambda)\mathrm{e}^{-ik} - 1}, \tag{A.3}$$

and the corresponding eigenvalue is

$$\epsilon(k) = \alpha + \beta + \gamma + \delta - 2\sqrt{(\gamma \mathrm{e}^{\lambda} + \beta)(\alpha \mathrm{e}^{-\lambda} + \delta)} \cos k. \tag{A.4}$$

$y(\lambda) < 1$ In addition to the above continuous spectrum a discrete band appears with

$$|\psi'(0)\rangle = \sqrt{1-y^2}\sum_{n=0}^{\infty} y^n |n\rangle \quad \text{and } \epsilon(0) = \alpha + \delta - (\beta+\gamma)\, y^2. \tag{A.5}$$

Here this is the lowest eigenvalue, correspondingly the spectrum becomes gapped. Notice that $\epsilon(k \to 0) \neq \epsilon(0)$.

We note that it is easy to prove that the above set is complete, i.e.,

$$\delta_{m,n} = \begin{cases} \int_0^\pi \langle m|\psi'(k)\rangle\langle\psi'(k)|n\rangle \,\mathrm{d}k & y(\lambda) > 1 \\ \int_0^\pi \langle m|\psi'(k)\rangle\langle\psi'(k)|n\rangle \,\mathrm{d}k + \langle m|\psi'(0)\rangle\langle\psi'(0)|n\rangle & y(\lambda) < 1 \end{cases} \tag{A.6}$$

The right and left eigenvectors $|\psi(k)\rangle$ and $\langle\psi(k)|$ of $\tilde{H}(\lambda)$ can be obtained by applying the operator Φ:

$$|\psi(k)\rangle = \Phi^{-1}|\psi'(k)\rangle, \quad \langle\psi(k)| = \langle\psi'(k)|\Phi. \tag{A.7}$$

for $k \in [0, \pi]$. In summary, for the lowest eigenvalue $\epsilon_0(\lambda)$ (infimum of the spectrum) of $\tilde{H}(\lambda)$ we obtain

$$\epsilon_0(\lambda) = \begin{cases} \alpha + \delta - (\beta+\gamma)\, y(\lambda)^2 & y(\lambda) > 1 \\ \alpha + \beta + \gamma + \delta - 2\,(\beta+\gamma)\, y(\lambda) & y(\lambda) < 1 \end{cases} . \tag{A.8}$$

It can easily be seen that this expression satisfies the symmetry relation (21), since $y(\lambda) = y(E-\lambda)$ with $\mathrm{e}^E = (\alpha\beta)\,/\,(\gamma\delta)$.

A.2. Calculation of the large deviation function

As a first step we write

$$\langle s|\mathrm{e}^{-\tilde{H}t}|P_0\rangle = (1-x)\sum_m \sum_n x^n \langle m|\mathrm{e}^{-\tilde{H}t}|n\rangle, \tag{A.9}$$

where $\langle m|$ is a row vector with a '1' at the mth position and '0's elsewhere. Inserting a complete set of eigenvectors we can write this in the form

$$\begin{aligned}\langle s|\mathrm{e}^{-\tilde{H}t}|P_0\rangle = {} & (1-x)\sum_m \sum_n x^n \int_0^\pi \langle m|\psi(k)\rangle\langle\psi(k)|n\rangle \mathrm{e}^{-\epsilon(k)t}\,\mathrm{d}k \\ & + \theta\,(1-y)\,(1-x)\sum_m \sum_n x^n \langle m|\psi(0)\rangle\langle\psi(0)|n\rangle \mathrm{e}^{-\epsilon(0)t}\end{aligned} \tag{A.10}$$

Here θ denotes the Heaviside function. Using the $k \to -k$ symmetry of the eigenvectors and eigenvalues in the contribution of the continuous part, the above integral can be rewritten in the form

$$\int_0^\pi \langle m|\psi(k)\rangle\langle\psi(k)|n\rangle \mathrm{e}^{-\epsilon(k)t}\,\mathrm{d}k = \frac{1}{2\pi}\phi^{n-m}\int_0^{2\pi}\left(\mathrm{e}^{\mathrm{i}k(n-m)} - \mathrm{e}^{2\mathrm{i}\varphi}\mathrm{e}^{\mathrm{i}k(n+m)}\right)\mathrm{e}^{-\epsilon(k)t}\,\mathrm{d}k. \tag{A.11}$$

After the substitution $z = \mathrm{e}^{\mathrm{i}k}$ and using (A.3) we obtain

$$\begin{aligned}\langle s|\mathrm{e}^{-\tilde{H}t}|P_0\rangle = {} & (1-x)\sum_m \sum_n x^n \phi^{n-m} \frac{1}{2\pi\mathrm{i}} \oint_{|z|=1} \left(z^{n-m-1} + \frac{yz-1}{z-y} z^{n+m}\right)\mathrm{e}^{-\varepsilon(z)t}\,\mathrm{d}z \\ & + \theta\,(1-y)\,(1-x)\sum_m \sum_n x^n \phi^{n-m}\left(1-y^2\right) y^{n+m}\mathrm{e}^{-\epsilon(0)t},\end{aligned} \tag{A.12}$$

where by $\varepsilon(z)$ we mean $\epsilon(k(z))$ based on the above substitution. In order to be able to perform the infinite sums in (A.12), we have to choose the contour of the integral carefully. In the first term of the integral there is a pole only at $z = 0$. Here we chose the contour to be a circle of radius $\phi^{-1} < |z| < (\phi x)^{-1}$ (denoted by C_1). In the second term we deform the contour to run along a circle around the origin with infinitesimal radius (denoted by C_2). Notice that doing so, for $y < 1$ we pick up a pole contribution at $z = y$, which just cancels with the last term in (A.12) (since $\epsilon(0) = \varepsilon(y)$). Finally we obtain

$$\begin{aligned}\langle s|\mathrm{e}^{-\tilde{H}t}|P_0\rangle = &-\frac{1-x}{2\pi\mathrm{i}x\phi}\oint_{C_1}\frac{\mathrm{e}^{-\varepsilon(z)t}}{\left(z-\frac{1}{x\phi}\right)\left(z-\frac{1}{\phi}\right)}\,\mathrm{d}z\\ &+\frac{1-x}{2\pi\mathrm{i}x}\oint_{C_2}\frac{(yz-1)\,\mathrm{e}^{-\varepsilon(z)t}}{\left(z-\frac{1}{x\phi}\right)(z-\phi)\,(z-y)}\,\mathrm{d}z. \qquad \text{(A.13)}\end{aligned}$$

To obtain the large deviation function we need to study the limit of this integral as $t \to \infty$. This enables us to build up the phase diagram as shown in section 4.1.

References

[1] R. J. Harris, A. Rákos, and G. M. Schütz. Breakdown of Gallavotti-Cohen symmetry for stochastic dynamics. *Europhys. Lett.*, 75(2):227–233, 2006.

[2] C. Giardinà, J. Kurchan, and L. Peliti. Direct evaluation of large-deviation functions. *Phys. Rev. Lett.*, 96(12):120603, 2006.

[3] D. J. Evans and D. J. Searles. The fluctuation theorem. *Adv. Phys.*, 51(7):1529–1585, 2002.

[4] F. Ritort. Work fluctuations, transient violations of the second law and free-energy recovery methods: Perspectives in theory and experiments. *Sém. Poincaré*, 2:195–229, 2003.

[5] J. Kurchan. Non-equilibrium work relations. *J. Stat. Mech.*, P07005, 2007.

[6] R. J. Harris and G. M. Schütz. Fluctuation theorems for stochastic dynamics. *J. Stat. Mech.*, P07020, 2007.

[7] D. J. Evans, E. G. D. Cohen, and G. P. Morriss. Probability of second law violations in shearing steady states. *Phys. Rev. Lett.*, 71(15):2401–2404, 1993.

[8] G. Gallavotti and E. G. D. Cohen. Dynamical ensembles in nonequilibrium statistical mechanics. *Phys. Rev. Lett.*, 74(14):2694–2697, 1995.

[9] G. Gallavotti and E. G. D. Cohen. Dynamical ensembles in stationary states. *J. Stat. Phys.*, 80(5–6):931–970, 1995.

[10] J. Kurchan. Fluctuation theorem for stochastic dynamics. *J. Phys. A: Math. Gen.*, 31(16):3719–3729, 1998.

[11] J. L. Lebowitz and H. Spohn. A Gallavotti-Cohen-type symmetry in the large deviation functional for stochastic dynamic. *J. Stat. Phys.*, 95(1–2):333–365, 1999.

[12] J. Kurchan. Gallavotti-Cohen theorem, chaotic hypothesis and the zero-noise limit. *J. Stat. Phys.*, 128(6):1307–1320, 2007.

[13] O. Narayan and A. Dhar. Reexamination of experimental tests of the fluctuation theorem. *J. Phys. A: Math. Gen.*, 37(1):63–76, 2004.

[14] F. Zamponi. Is it possible to experimentally verify the fluctuation relation? A review of theoretical motivations and numerical evidence. *J. Stat. Mech.*, P02008, 2007.

[15] S. Schuler, T. Speck, C. Tietz, J. Wrachtrup, and U. Seifert. Experimental test of the fluctuation theorem for a driven two-level system with time-dependent rates. *Phys. Rev. Lett.*, 94(18):180602, 2005.

[16] C. Tietz, S. Schuler, T. Speck, U. Seifert, and J. Wrachtrup. Measurement of stochastic entropy production. *Phys. Rev. Lett.*, 97(5):050602, 2006.

[17] R. van Zon and E. G. D. Cohen. Extension of the fluctuation theorem. *Phys. Rev. Lett.*, 91(11):110601, 2003.

[18] N. Garnier and S. Ciliberto. Nonequilibrium fluctuations in a resistor. *Phys. Rev. E*, 71(6):060101(R), 2005.

[19] M. Dolowschiák and Z. Kovács. Fluctuation formula in the Nosé-Hoover thermostated lorentz gas. *Phys. Rev. E*, 71(2):025202(R), 2005.

[20] F. Bonetto, G. Gallavotti, A. Giuliani, and F. Zamponi. Chaotic hypothesis, fluctuation theorem and singularities. *J. Stat. Phys.*, 123(1):39–54, 2006.

[21] A. Puglisi, L. Rondoni, and A. Vulpiani. Relevance of initial and final conditions for the fluctuation relation in Markov processes. *J. Stat. Mech.*, P08010, 2006.

[22] P. Visco. Work fluctuations for a Brownian particle between two thermostats. *J. Stat. Mech.*, P06006, 2006.

[23] R. van Zon and E. G. D. Cohen. Extended heat-fluctuation theorems for a system with deterministic and stochastic forces. *Phys. Rev. E*, 69(5):056121, 2004.

[24] J. Farago. Injected power fluctuations in Langevin equation. *J. Stat. Phys.*, 107(3–4):781–803, 2002.

[25] M. Baiesi, T. Jacobs, C. Maes, and N. S. Skantzos. Fluctuation symmetries for work and heat. *Phys. Rev. E*, 69(2):021111, 2006.

[26] T. Taniguchi and E. G. D. Cohen. Onsager-Machlup theory for nonequilibrium steady states and fluctuation theorems. *J. Stat. Phys.*, 126(1):1–41, 2007.

[27] G. M. Schütz. Exactly solvable models for many-body systems far from equilibrium. In C. Domb and J. Lebowitz, editors, *Phase Transitions and Critical Phenomena*, volume 19. London: Academic Press, 2001.

[28] D. J. Evans and D. J. Searles. Equilibrium microstates which generate second law violating steady states. *Phys. Rev. E*, 50(2):1645–1648, 1994.

[29] D. J. Searles and D. J. Evans. Fluctuation theorem for stochastic systems. *Phys. Rev. E*, 60(1):159–164, 1999.

[30] F. Spitzer. Interaction of Markov processes. *Adv. Math.*, 5(2):246–290, 1970.

[31] M. R. Evans and T. Hanney. Nonequilibrium statistical mechanics of the zero-range process and related models. *J. Phys. A: Math. Gen.*, 38(19):R195–R240, 2005.

[32] M. R. Evans. Phase transitions in one-dimensional nonequilibrium systems. *Braz. J. Phys.*, 30(1):42–57, 2000.

[33] I. Jeon, P. March, and B. Pittel. Size of the largest cluster under zero-range invariant measures. *Ann. Probab.*, 28(3):1162–1194, 2000.

[34] G. M. Shim, B. Y. Park, J. D. Noh, and H. Lee. Analytic study of the three-urn model for separation of sand. *Phys. Rev. E*, 70(3):031305, 2004.

[35] E. Levine, D. Mukamel, and G. M. Schütz. Zero-range process with open boundaries. *J. Stat. Phys.*, 120(5–6):759–778, 2005.

[36] R. J. Harris, A. Rákos, and G. M. Schütz. Current fluctuations in the zero-range process with open boundaries. *J. Stat. Mech.*, P08003, 2005.

[37] T. Bodineau and B. Derrida. Current fluctuations in non-equilibrium diffusive systems: an additivity principle. *Phys. Rev. Lett.*, 92(18):180601, 2004.

[38] F. van Wijland and Z. Rácz. Large deviations in weakly interacting boundary driven lattice gases. *J. Stat. Phys.*, 118(1–2):27–54, 2005.

[39] R. Juhász, L. Santen, and F. Iglói. Partially asymmetric zero-range process with quenched disorder. *Phys. Rev. E*, 72:046129, 2005.

[40] A. Dembo and O. Zeitouni. *Large Deviation Techniques and Applications.* Springer, 1998.

[41] Y. Oono. Large deviation and statistical physics. *Prog. Theor. Phys.*, 99:165–205, 1989.

[42] H. Touchette. The large deviation approach to statistical mechanics. arXiv:0804.0327, 2008.

[43] V. Lecomte, C. Appert-Rolland, and F. van Wijland. Thermodynamic formalism for systems with markov dynamics. *J. Stat. Phys.*, 127(1):51–106, 2007.

[44] V. Lecomte and J. Tailleur. A numerical approach to large deviations in continuous time. *J. Stat. Mech.*, P03004, 2007.

[45] O. Pulkkinen. Boundary driven zero-range processes in random media. *J. Stat. Phys.*, 128(6):1289–1305, 2007.

[46] B. Derrida, B. Douçot, and P.-E. Roche. Current fluctuations in the one-dimensional symmetric exclusion process with open boundaries. *J. Stat. Phys.*, 115(3-4):717–748, 2004.

[47] H. Touchette and E. G. D. Cohen. Fluctuation relation for a Lévy particle. *Phys. Rev. E*, 76:020101(R), 2007.